

The role of reinforced concrete roofs in the seismic performance of masonry buildings

*Original*

The role of reinforced concrete roofs in the seismic performance of masonry buildings / Cardoni, A.; Cimellaro, G. P.. - In: JOURNAL OF BUILDING ENGINEERING. - ISSN 2352-7102. - ELETTRONICO. - 28:(2020), p. 101056. [10.1016/j.jobe.2019.101056]

*Availability:*

This version is available at: 11583/2840451 since: 2021-10-29T11:16:54Z

*Publisher:*

Elsevier

*Published*

DOI:10.1016/j.jobe.2019.101056

*Terms of use:*

This article is made available under terms and conditions as specified in the corresponding bibliographic description in the repository

*Publisher copyright*

Elsevier postprint/Author's Accepted Manuscript

© 2020. This manuscript version is made available under the CC-BY-NC-ND 4.0 license  
<http://creativecommons.org/licenses/by-nc-nd/4.0/>. The final authenticated version is available online at:  
<http://dx.doi.org/10.1016/j.jobe.2019.101056>

(Article begins on next page)

# The role of reinforced concrete roofs in the seismic performance of masonry buildings

Alessandro Cardoni<sup>a</sup>, Gian Paolo Cimellaro<sup>b,\*</sup>

<sup>a</sup>PhD Student, Department of Structural, Geotechnical and Building Engineering, Politecnico di Torino, Corso Duca degli Abruzzi 24, 10129, Turin, Italy. E-mail: [alessandro.cardoni@polito.it](mailto:alessandro.cardoni@polito.it)

<sup>b</sup>Associate Professor, Department of Structural, Geotechnical and Building Engineering, Politecnico di Torino, Corso Duca degli Abruzzi 24, 10129, Turin, Italy. E-mail: [gianpaolo.cimellaro@polito.it](mailto:gianpaolo.cimellaro@polito.it)

\*Corresponding author. Tel.: +39 011 0904801. E-mail: [gianpaolo.cimellaro@polito.it](mailto:gianpaolo.cimellaro@polito.it)

## Abstract

The 2016 Central Italy earthquake caused many collapses of existing masonry buildings that had previously been retrofitted with reinforced concrete roofs. The aim of this paper is to explore the role of these roofs in the seismic behaviour of masonry buildings. Simple analytical models are presented to illustrate two typical out-of-plane collapse mechanisms: wall overturning and vertical flexure. The models are based on linear kinematic analysis, which allows fast modelling and calculation of a coefficient that can be used to assess the safety level of a structure. Nonlinear kinematic analyses were also performed. Both methods were applied to two case studies taken from areas struck by the earthquake. Results show that linear analysis represents an effective tool for preliminary verifications that can allow one to understand whether retrofit interventions are needed.

Keywords: masonry, reinforced concrete roof, collapse, retrofit, kinematic analysis, Central Italy earthquake

## 1. Introduction

After the 24<sup>th</sup> August 2016 Central Italy earthquake, most of the buildings of small towns nearby the epicenter were declared unsafe and several structures collapsed completely. Poor material quality and scant building techniques were certainly the main reason of collapses. However, inadequate retrofit interventions also contributed to the disruptive effect of the seismic event. For instance, the replacement of the old wooden roofs with reinforced concrete roofs seemed to facilitate some mechanisms that led to severe damages and collapses. This type of retrofitting was broadly adopted in the 80s and 90s since it was believed to be effective against seismic actions. In fact, it was the Italian code itself to recommend it [1]. Moreover, at that period there was a massive use of concrete that led to a gradual abandon of research and experimental tests on masonry [2]. The overall idea was to put robust structures such as RC roofs and floors connected to perimetric walls by means of RC ring beams to avoid independent movements of masonry macro-elements. After Tolmezzo earthquake in 1976, this and other retrofitting techniques became part of technical codes, until Umbria and Marche earthquake in 1997 [3, 4].

40 This event pointed out the disadvantages of heavy and stiff roofs and floors. In fact, if vertical  
41 structures are not robust enough, they are indeed the primary cause of collapses. The significant  
42 stiffness and load increment at the top have led to the collapse of the walls, which were made of  
43 poor materials and not strengthened. Conversely, there were also many cases of masonry  
44 structures retrofitted with reinforced concrete roofs that withstood the earthquake with no  
45 significant damages (Figure 1).



46  
47 Figure 1. Masonry buildings retrofitted with concrete roof not collapsed after the earthquake in  
48 Pescara del Tronto (a-b) and small villages near Accumoli (c-d).

49  
50 However, there is no guarantee that those buildings are safe. Therefore, in this paper a simple  
51 verification procedure that is able to estimate the level of safety of masonry buildings with  
52 reinforced concrete roofs is implemented. The adopted approach is based on the linear kinematic  
53 analysis, which is also described by Italian codes [5, 6]. Despite the method is well known in its  
54 theoretical formulation, it is rarely used and usually the effect of the roof and the connection  
55 among structural elements are neglected. This research contributes to the current literature with  
56 practical applications of the kinematic analysis introducing simplified analytical models that  
57 take into account the effect of reinforced concrete roofs. An additional advantage of the  
58 proposed models is that the number of input parameters has been reduced as much as possible so  
59 that the analysis does not require any particular investigation or survey to be carried out. A  
60 safety factor was also defined to assess the safety level of the building towards different collapse

61 mechanisms. The choice of a simplified procedure has been made in order to have a fast tool  
62 which could be used even by non-professional users. The method would allow property owners  
63 to understand if they are in danger. For instance, if the obtained safety factor is low or close to  
64 the unsafe threshold, further investigations should be conducted. More detailed methods have  
65 been studied by many authors to describe masonry buildings behaviour, but they need to be  
66 calibrated and the input data are often not accessible [7-10]. Obviously, results will not be as  
67 accurate, and a certain margin of error should be taken into account in final considerations.  
68 Nonetheless, they can provide relevant preliminary information about the structure. In addition,  
69 in the literature there is a number of studies about masonry where analytical models turned out  
70 to be highly effective and close to the real behaviour [11, 12].

71 After defining the formulation, the method is applied to different models describing the  
72 overturning and the vertical flexural behaviour. The models derive from those commonly used  
73 to study the out-of-plane mechanisms [13-15] and the arch rocking [16-18]. To analyse the  
74 influence of the connection between the roof and the floor to the walls, a ring beam is also  
75 considered. The presence of a reinforced concrete (RC) ring beam is dangerous if it is not well  
76 connected to masonry walls and if the latter is not strengthened. Furthermore, the spread of  
77 reinforced concrete in the construction sector, led to wrong applications in the interventions of  
78 existing buildings. Nowadays there are many solutions to realize effective structural  
79 connections, such as reinforced masonry ring beams [19]. The use of innovative composite  
80 materials has become a common practice in retrofit strategies. Several studies have been carried  
81 out in this field which has allowed to investigate the behavior of strengthened beams [20, 21]  
82 and strengthened masonry walls through out-of-plane tests [22].

83 Two case studies taken from two towns struck by the abovementioned earthquake were  
84 analyzed, but the method can be extended to any building by choosing appropriate parameters.  
85 Both examples were selected by considering typical houses in the area, built with local materials  
86 and poor construction techniques and retrofitted with reinforced concrete roofs. The first one is  
87 1-storey building while the second one has two storeys and thus also the action of the inter-  
88 storey floor is considered in the model. For each model, the linear kinematic analysis is repeated  
89 for different values of the input parameters, as they could be affected by uncertainty. In this way  
90 it is possible to see the influence of a single parameter and what happens if it is over-estimated  
91 or under-estimated. Finally, nonlinear analyses are performed in order to compare the results and  
92 understand if the additional computational effort of a more refined method is worth it.

93

## 94 **2. The linear kinematic analysis**

95 In existing masonry buildings there are often collapses due to a loss of equilibrium of some  
96 portions of bearing structures. In general, these types of mechanisms happen when seismic  
97 forces act in the out-of-plane direction. The linear kinematic analysis can be used to study  
98 these phenomena and for the verification process. It is based on the choice of the possible  
99 mechanisms that are most likely to happen. These ones are assumed by evaluating the current  
100 cracking state and analyses performed on similar buildings. In the literature there are plenty  
101 of studies on historical buildings, such as churches, which are helpful to clarify how the  
102 collapse process activates and evolve [23]. The ability to detect the most probable  
103 mechanisms is crucial to prevent local or global collapses, since it is possible to run specific  
104 analyses and consequently suggest specific interventions.

105 The linear kinematic approach schematizes the building in a discrete number of macro-  
 106 elements which move according to their boundary conditions. For this reason, the  
 107 assumptions are that the material has no tensile strength and infinite compressive strength. In  
 108 each rigid block, vertical loads (including dead and external loads) and a system of horizontal  
 109 forces are applied. Horizontal forces are proportional to the vertical loads through a  
 110 coefficient called load multiplier ( $\alpha$ ). Incrementing the load multiplier, it is possible to  
 111 evaluate the horizontal force that activates a specific mechanism.  $\alpha_C$  is named the collapse  
 112 load multiplier, and it is calculated with the principle of virtual works. Therefore, the total  
 113 work of the external forces ( $L_e$ ) has to be equal to the total work of the internal forces ( $L_i$ )  
 114 which in this case is null as shown in Eq. (1):

$$115 \quad L_e = \alpha_C \left( \sum_{i=1}^n W_i \cdot \delta_{x,i} + \sum_{j=n+1}^{n+m} W_j \cdot \delta_{x,j} \right) - \sum_{i=1}^n W_i \cdot \delta_{y,i} - \sum_{h=1}^o F_h \cdot \delta_h = L_i = 0 \quad (1)$$

116 where:  $n$  is the number of the weight forces applied to all macro-elements;  $m$  is the number of  
 117 weight forces that generate horizontal forces upon macro-elements;  $o$  is the number of  
 118 external forces;  $W_i$  is the generic weight force;  $W_j$  is the generic weight force that generates  
 119 horizontal forces upon macro-elements;  $\delta_{x,i}$  is the virtual horizontal displacement of the point  
 120 where the  $i$ -th weight force is applied;  $\delta_{y,i}$  is the virtual vertical displacement of the point  
 121 where the  $i$ -th weight force is applied;  $F_h$  is the generic external force;  $\delta_h$  is the virtual  
 122 displacement of the point where the generic external force  $F_h$  is applied. Eq. (1) often  
 123 becomes an equilibrium equation between a stabilizing moment and an overturning moment,  
 124 so it is not necessary to calculate the virtual displacement. The method is also used to  
 125 determine the most probable collapse mechanism which is the one that requires less energy to  
 126 be activated (i.e. the one with the lower load multiplier). However, the decay conditions of  
 127 masonry should never be neglected since they are able to reveal if a specific mechanism has  
 128 already been activated. Once  $\alpha_C$  is calculated, it is possible to obtain the acceleration that  
 129 generates the mechanism (Eq. (2)).

$$130 \quad a_0^* = \frac{\alpha_C \cdot \sum_{i=1}^{n+m} P_i}{M^* \cdot FC} \quad (2)$$

131 where  $FC$  is a coefficient that depends on the level of knowledge about the masonry  
 132 structure. The level of knowledge is based on information like geometry, construction details,  
 133 and material properties. Such data can be acquired in different ways, from generic research  
 134 and visual inspection to extensive tests and measurements. Since the material strength is not  
 135 considered in this research, only basic information about geometric characteristics, type of  
 136 masonry panels and construction details was collected. According to the Italian code [6],  
 137 three level of knowledge can be identified: limited, extended and exhaustive. Due to the  
 138 limited available data, the level of knowledge is limited. In this case, the code reports the  $FC$   
 139 coefficient has to be assumed equal to 1,35 which reduces the acceleration that generates the  
 140 mechanism.  $M^*$  is the participating mass, calculated considering the virtual displacements of  
 141 the points where the loads are applied, as shown in Eq. (3) [6]:

142

$$M^* = \frac{\left( \sum_{i=1}^{n+m} P_i \cdot \delta_{x,i} \right)^2}{g \cdot \sum_{i=1}^{n+m} P_i \cdot \delta_{x,i}^2} \quad (3)$$

143 The acceleration given by Eq. (2) has now to be compared with an allowable acceleration.  
 144 This one is given by Eq. (4), which is valid when the analysed blocks are in contact with the  
 145 ground, meaning that the mechanism involves ground floor walls:

146

$$a^* = \frac{a_g \cdot S}{q} \quad (4)$$

147 where:  $a_g$  is the peak ground acceleration at the site determined, as indicated by Italian codes,  
 148 for a return period of 475 years;  $q$  is the reduction factor which can be assumed equal to 2 for  
 149 regular masonry structures;  $S$  is given by the product of two coefficients:  $S_s$  that depends on  
 150 the soil category and represents the stratigraphic amplification, and  $S_t$  which takes into  
 151 account the effects of the topographical amplification and depends on the surface  
 152 configuration of the soil.

153 It is clear that the acceleration that activates the mechanism should be greater than the  
 154 allowable one. To quickly verify this, it is possible to introduce a safety factor which is the  
 155 ratio between the two accelerations (Eq. (5)):

156

$$SF = \frac{a_0^*}{a^*} \geq 1 \quad (5)$$

157

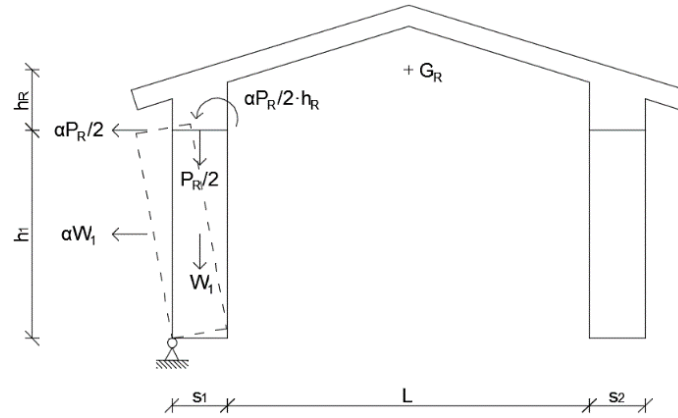
### 158 3. Analytical models

159 In some cases, there are mechanisms that are suggested by the building itself just looking to  
 160 the geometry, the nature of the structural elements, the cracking state, the interventions  
 161 occurred over the years, etc. The linear kinematic analysis is a powerful tool that can be used  
 162 to describe local mechanisms that have been observed after disruptive earthquakes. If only  
 163 out-of-plane mechanisms are considered, then they can be basically grouped in three  
 164 categories: (i) overturning, (ii) vertical flexural behaviour and (iii) horizontal flexural  
 165 behaviour. In this paper only the first two categories are considered since they were the main  
 166 cause of collapses during the Central Italy earthquake. In addition, for these two mechanisms  
 167 the presence of a reinforced concrete roof is more crucial. For the overturning, two cases  
 168 were studied, a 1-storey and a 2-storey building, whereas for the vertical flexural behaviour  
 169 only the 2-storey building was studied, taking into account also the effect of the inter-storey.  
 170 The considered macro-elements are the walls, the floor, and the reinforced concrete roof. This  
 171 one is assumed as an element that transfers only vertical loads to the walls and no lateral  
 172 thrusts. Therefore, it is modelled as a rigid block with a large mass. The effects of  
 173 perpendicular walls are neglected, as in many real cases there are no connections. All models  
 174 consider alternatively the presence and the absence of connections between roof and walls  
 175 (by means of a ring beam) and between floor and walls. When there is a ring beam the roof is  
 176 fixed to the walls and moves with them, while when there is no connection the roof is  
 177 considered simply supported.

178

### 179 3.1 1-storey overturning without ring beam

180 This is the case of simple overturning where there is no ring beam, and therefore no  
 181 connection between the top of the wall and the roof. For this reason, the macro-elements are  
 182 independent one from another and only one wall is subjected to overturning. Figure 2  
 183 illustrates the mechanism and the forces involved.  $W_l$  is the weight of the left wall,  $P_R$  is the  
 184 weight of the roof applied in its center of mass  $G_R$  and split equally between the two walls.



185

186 Figure 2. Calculating scheme for 1-storey overturning without ring beam.

187

188 According to Eq. (1) the load multiplier that leads to collapse for this configuration is given  
 189 by Eq. (6):

$$190 \quad \alpha_C = \frac{W_l \cdot \frac{s_1}{2} + \frac{P_R}{2} \cdot \frac{s_1}{2}}{W_l \cdot \frac{h_1}{2} + \frac{P_R}{2} \cdot (h_1 + h_R)} \quad (6)$$

191 where  $s_l$  is the thickness of left wall;  $h_l$  is the height of walls;  $h_R$  is the distance between the  
 192 top of walls and the center of mass ( $G_R$ ) of the roof, and  $L$  is the span length.

193

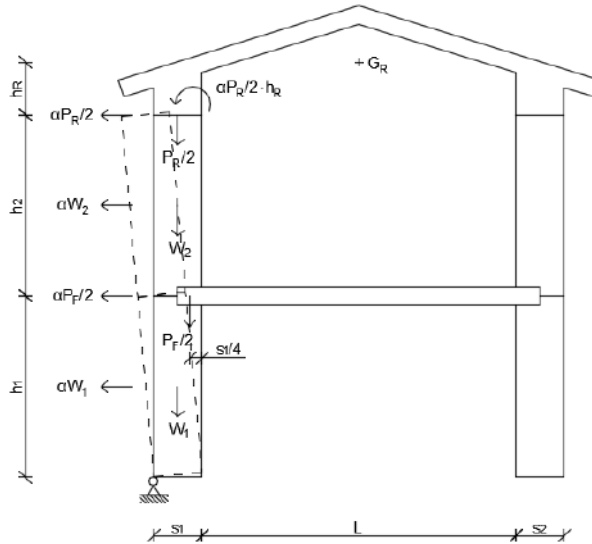
### 194 3.2 1-storey overturning with ring beam

195 If there is a ring beam the two external walls are connected at the top to realize the so called  
 196 “box-like” behaviour. Macro-elements are no more independent, so they move together until  
 197 the loss of equilibrium. As shown in Figure 3 both walls rotate around the hinge at the bottom  
 198 under a seismic action. The effect of the ring beam is modelled using a force acting in the  
 199 opposite direction of the kinematic movement. To a first approximation, it can be calculated  
 200 as the product of the friction coefficient  $\mu$  and the weight of the roof  $P_R$ . For the estimation of  
 201 the friction coefficient there are many experimental tests available in literature [24].

202 However, since the proposed model is simplified and no detailed information about the  
 203 materials were available, the guidelines provided by national codes were followed [5, 6]. In  
 204 particular, as a precautionary measure, a friction coefficient of 0.4 was used, which is the  
 205 lowest among the suggested values.







225

226

Figure 4. Calculating scheme for 2-storey overturning without ring beam.

227

### 228 3.4 2-storey overturning with ring beam

229

230

231

232

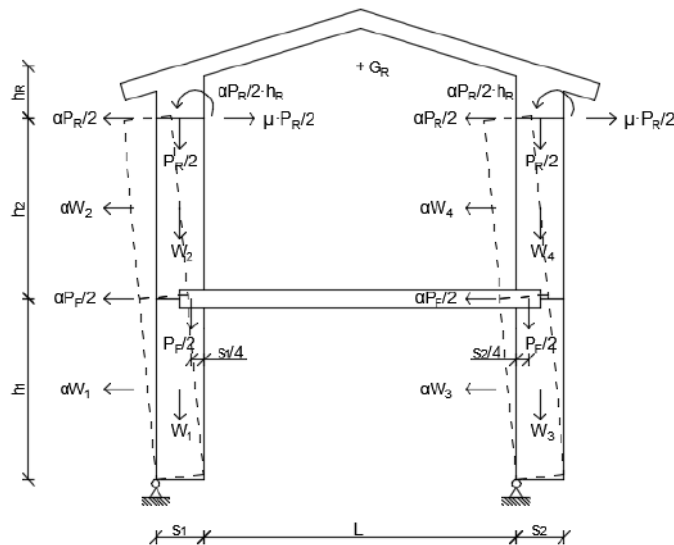
233

As already seen in the 1-storey case, the ring beam at the roof level connects the walls together, so they can overturn at the same time. Once again, the connection is modelled as a friction force proportional to the weight of the roof (Figure 5). In this case, the inter-storey floor is well connected to the walls and moves together with them. Eq. (9) provides the collapse load multiplier for this case:

$$234 \quad \alpha_c = \frac{\left(W_1 + W_2 + \frac{P_R}{2}\right) \cdot \frac{s_1}{2} + \frac{P_F}{2} \cdot \frac{3s_1}{4} + \left(W_3 + W_4 + \frac{P_R}{2}\right) \cdot \frac{s_2}{2} + \frac{P_F}{2} \cdot \frac{s_2}{4} + (\mu \cdot P_R) \cdot (h_1 + h_2)}{\left(W_1 + W_3\right) \cdot \frac{h_1}{2} + P_F \cdot h_1 + \left(W_2 + W_4\right) \cdot \left(h_1 + \frac{h_2}{2}\right) + P_R \cdot (h_1 + h_2) + P_R \cdot h_R} \quad (9)$$

235

where  $W_4$  is the weight of the right masonry panel of the upper level.



236

237

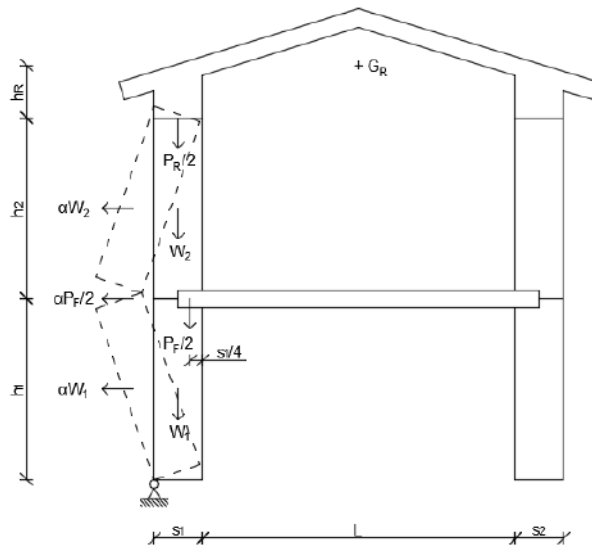
Figure 5. Calculating scheme for 2-storey overturning with ring beam.

238

239 **3.5 2-storey flexural behaviour without connection between floor and walls**

240 Vertical flexural behaviour can occur in any part of the wall. It can be seen as a triple-hinged  
 241 arch where, in this specific case, the hinges are located at the bottom, at the top, and at the  
 242 inter-storey level. This means that the mechanism is activated by the horizontal inertial force  
 243 caused by the floor during the seismic action. The upper level wall is connected at the top of  
 244 the roof, whereas the inter-storey floor is not connected to the walls (Figure 6). The collapse  
 245 load multiplier  $\alpha_C$  is given by Eq. (10):

246 
$$\alpha_C = \frac{W_1 \cdot \frac{s_1}{2} + W_2 \cdot \left( s_1 + \frac{s_1}{2} \cdot \frac{h_1}{h_2} \right) + \frac{P_F}{2} \cdot \frac{3s_1}{4} + \frac{P_R}{2} \cdot \left( s_1 + \frac{s_1}{2} \cdot \frac{h_1}{h_2} \right)}{W_1 \cdot \frac{h_1}{2} + W_2 \cdot \left( h_1 \cdot \frac{h_1}{h_2} + \frac{h_2}{2} \cdot \frac{h_1}{h_2} \right) + \frac{P_F}{2} \cdot h_1} \quad (10)$$



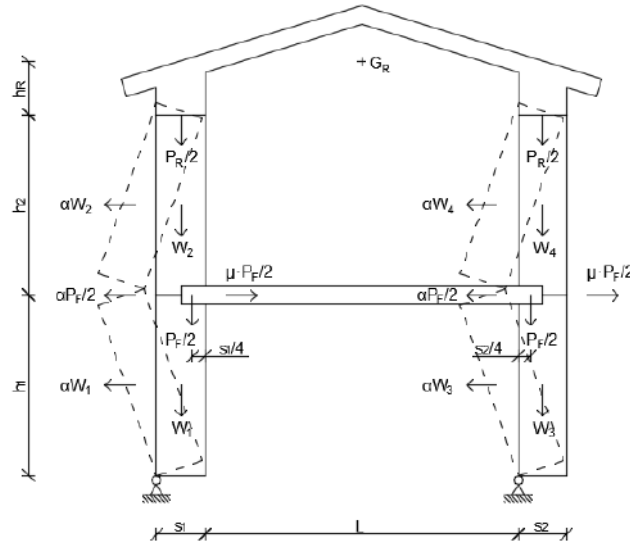
247

248 Figure 6. Calculating scheme for vertical flexural behaviour without floor-walls connection.

249

250 **3.6 2-storey flexural behaviour with connection between floor and walls**

251 In this model the floor is well connected to the walls so that it can pull them together, but  
 252 eventually it detaches. To represent this type of connection, a friction force proportional to  
 253 the floor weight is considered at the inter-storey level (Figure 7).



254

255 Figure 7. Calculating scheme for vertical flexural behaviour with floor-walls connection.

256

257 Eq. (11) allows to get the collapse load multiplier for this model:

$$\begin{aligned}
 \alpha_C = & \frac{W_1 \cdot \frac{s_1}{2} + W_2 \cdot \left( s_1 + \frac{s_1}{2} \cdot \frac{h_1}{h_2} \right) + W_3 \cdot \frac{s_2}{2} + W_4 \cdot \left( s_2 + \frac{s_2}{2} \cdot \frac{h_1}{h_2} \right) + \frac{P_F}{2} \cdot \frac{3s_1}{4} + \frac{P_F}{2} \cdot \frac{s_2}{4}}{ \\
 & (W_1 + W_3) \cdot \frac{h_1}{2} + (W_2 + W_4) \cdot \left( h_1 \cdot \frac{h_1}{h_2} + \frac{h_2}{2} \cdot \frac{h_1}{h_2} \right) + P_F \cdot h_1} + \\
 & \frac{\frac{P_R}{2} \cdot \left( s_1 + \frac{s_1}{2} \cdot \frac{h_1}{h_2} \right) + \frac{P_R}{2} \cdot \left( s_2 + \frac{s_2}{2} \cdot \frac{h_1}{h_2} \right) + (\mu \cdot P_F) \cdot h_1}{ \\
 & (W_1 + W_3) \cdot \frac{h_1}{2} + (W_2 + W_4) \cdot \left( h_1 \cdot \frac{h_1}{h_2} + \frac{h_2}{2} \cdot \frac{h_1}{h_2} \right) + P_F \cdot h}
 \end{aligned} \tag{11}$$

259

## 260 4. Case studies

### 261 4.1 Pescara del Tronto case study

262 Figure 8 shows a house in Pescara del Tronto completely collapsed after the 2016 Central  
 263 Italy earthquake, which can be used as an example to apply the 1-storey model. The data that  
 264 were used as input in the model are the following: wall thickness ( $s = s_1 = s_2$ ) = 0.4 m; roof  
 265 thickness ( $s_R$ ) = 0.15 m; wall height ( $h_1$ ) = 3 m; wall length ( $l_w$ ) = 7 m; span length ( $L$ ) = 5 m;  
 266 distance between the center of mass of the roof and the top of the wall ( $h_R$ ) = 0.4 m; specific  
 267 weight of masonry ( $P_m$ ) = 19 kN/m<sup>3</sup>; specific weight of reinforced concrete ( $P_c$ ) = 21 kN/m<sup>3</sup>;  
 268 friction coefficient roof – wall ( $\mu$ ) = 0.4; PGA for a return period of 475 years ( $a_g$ ) = 2.489  
 269 m/s<sup>2</sup>;  $S_s$  = 1 (rock soil);  $S_t$  = 1.2 (top of a hill). The weight of the walls was calculated as  
 270  $W_i = h_i \cdot l_w \cdot s_i \cdot P_m$ , where  $i=1, 2$ , while the weight of the roof as

$$271 \quad W_i = 2 \cdot \left[ \sqrt{(s + L/2)^2 + h_r^2} \cdot l_w \cdot s_r \cdot P_c \right].$$



Figure 8. View of the building used as case study before and after the earthquake.

272

273

274

275 As already mentioned, most of the data are geometrical so they can be easily collected. Only  
 276 the PGA needs to be calculated referring to the information given by the Italian code [5]. In  
 277 this case, the location is fixed, so the value can be determined analytically. The value used for  
 278  $S_s$  is referred to rock soil, while the one used for  $S_t$  is referred to the top of a hill as there is  
 279 evidence of a slope behind the building.

280

#### 281 4.1.1 Pescara del Tronto results

282 The results using the linear kinematic analysis and verification are reported in Table 1.

283

284 Table 1. Collapse load multipliers and safety factors for the Pescara del Tronto case study.

	1-storey overturning without ring beam	1-storey overturning with ring beam
$\alpha_c$	0.10	0.26
$SF$	0.57	1.48

285

286 Comparing the load multipliers, it can be observed that the first mechanism is more likely to  
 287 happen as the 1-storey overturning with ring beam case has a collapse load 2.6 times higher  
 288 than the 1-storey overturning without ring beam. This is confirmed by the fact that the safety  
 289 factor in the case without ring beam is lower and it is below the safety threshold. Indeed, as  
 290 shown in Figure 8 there is no connection between roof and walls. If this kind of analysis was  
 291 carried out in a pre-earthquake situation, it would have been possible to demonstrate how the  
 292 building was unsafe towards a seismic event with a return period of 475 years. The actual  
 293 demand of 2016 earthquake was larger than the one used as input for this verification  
 294 procedure. However, the aim of the method is to report if retrofitting is needed to improve the  
 295 level of safety. Validation analyses were not performed at this stage, but adequate  
 296 interventions could have likely prevented the structure from a complete collapse.

297 A sensitivity analysis was carried out to assess the impact of the chosen input parameters on  
 298 results. Most relevant outcomes were then plotted in graphs with the varying parameter on  
 299 the  $x$  axis and the safety factor  $SF$  on the  $y$  axis. Figure 9(a) shows that when there is no

300 friction the two mechanisms are equivalent because of the symmetry of the systems and the  
301 configuration is unsafe. The minimum friction coefficient to ensure a safety factor greater  
302 than 1 is 0.2. As predictable, the impact of the friction is overall positive: it is enough to build  
303 a ring beam able to ensure a friction coefficient of 0.4 and triple the safety factor. In Figure  
304 9(b) the span length is varying, resulting in an increase or decrease in the weight of the roof.  
305 This has almost no effects in the case without ring beam, which remains unsafe in the whole  
306 range of variation. On the other hand, since the friction force is proportional to the weight of  
307 the roof, increasing the span length leads to a significant increment of the safety factor. When  
308 the masonry specific weight of the masonry varies, safety factor remains almost constant  
309 (Figure 9(c)). The weight of the walls has indeed a twofold effect since it contributes to both  
310 stabilizing and overturning forces. Also, looking at the equations that lead to determine SF (in  
311 particular Eqs. (6-7) and Eq. (2)), it can be noticed how the weight appears always at both  
312 nominator and denominator. Therefore, in the calculation steps its variation tends to have  
313 negligible effects. Figure 9(d) shows the influence of the wall thickness. In the first case,  
314 without ring beam, an increment of the wall thickness corresponds to a linear and  
315 considerable increment of the  $SF$ . However, almost 70 cm walls are required to be in the safe  
316 area. In the second case, there is an asymptotic trend. It means that for low thicknesses the  
317 presence of the ring beam is effective (e.g. for  $s = 20$  cm the  $SF$  is two times the  $SF$  in the  
318 case with no ring beam), but for high thicknesses the structure is so massive that the presence  
319 of the ring beam at the top is irrelevant. Finally, in Figure 9(e) different soil categories are  
320 taken into account by varying the abovementioned parameter  $S_s$ . Following the guidelines  
321 provided by the Italian seismic codes, the possible values  $S_s$  can assume were calculated  
322 (Table 2). A rock soil allows to have higher safety factors, whereas if the quality gets worse  
323 there is a decreasing trend, except for category E (coarse soil upon a stiff or soft soil).

324

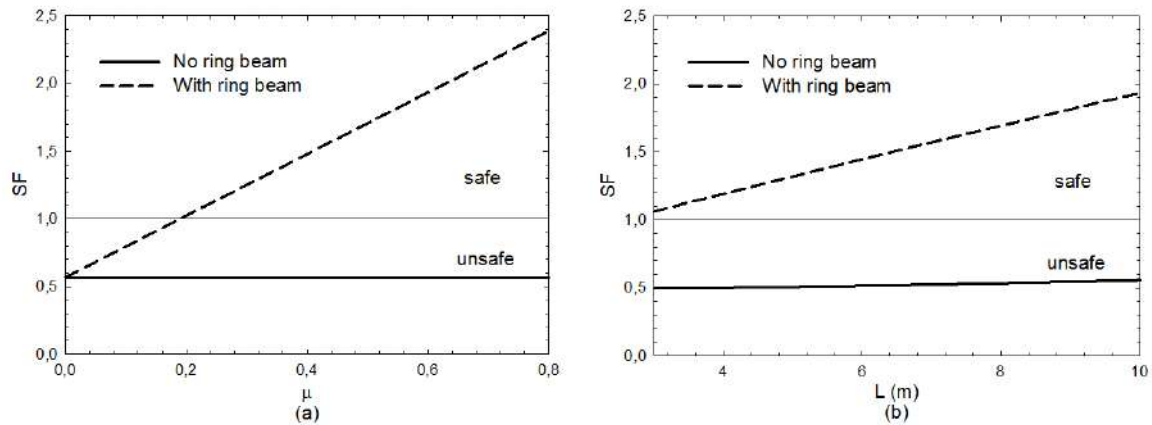
325 Table 2. Values of the parameter  $S_s$  for different soil categories.

Soil category	Description	$S_s$
A	Rock soil ( $V_{s30} > 800$ m/s)	1.00
B	Soft rock and very dense soil ( $360$ m/s $< V_{s30} < 800$ m/s)	1.16
C	Stiff soil ( $180$ m/s $< V_{s30} < 360$ m/s)	1.33
D	Soft soil ( $V_{s30} < 180$ m/s)	1.48
E	Coarse soil upon stiff or soft soil	1.33

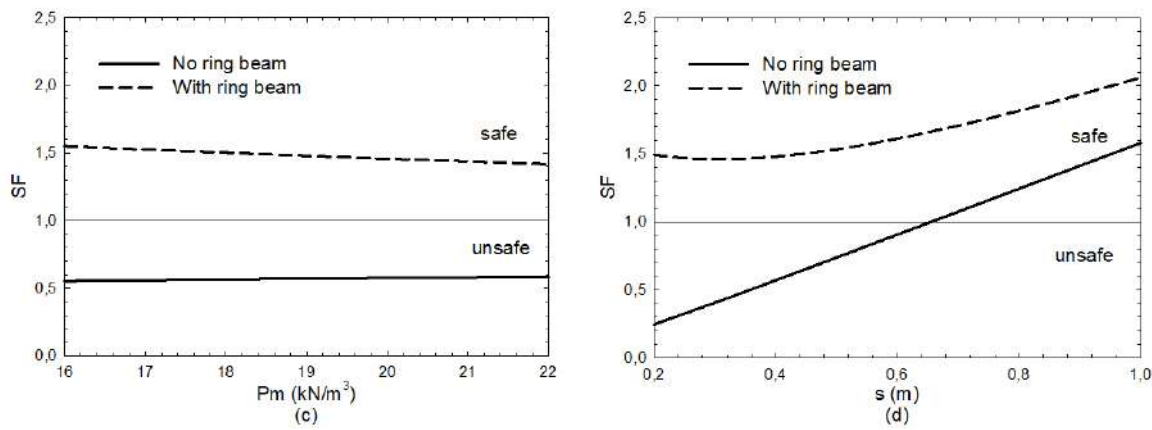
326

327

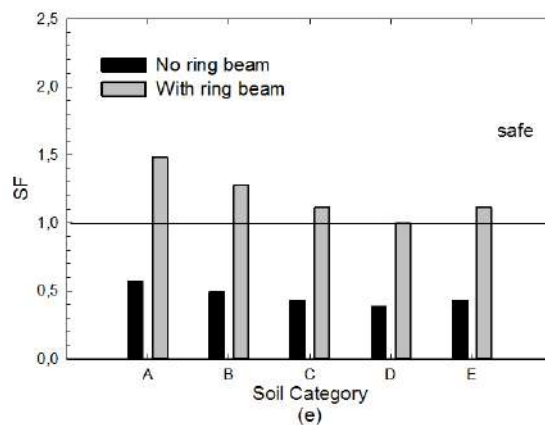
328



329



330



331 Figure 9. (a) Friction coefficient vs. safety factor, (b) span length vs. safety factor, (c)  
332 masonry specific weight vs. safety factor, (d) wall thickness vs. safety factor, (e) soil category  
333 vs. safety factor.

334

#### 335 4.2 Amatrice case study

336 The 2-floor models were tested through the building in Figure 10 which was located in  
337 Amatrice. The data used as input for the analysis are the following: wall thickness ( $s_1 = s_2$ ):  
338 0.4 m; roof thickness ( $s_R$ ): 0.15 m; wall height ( $h_1 = h_2$ ): 3 m; wall length ( $l_w$ ): 11 m; span  
339 length ( $L$ ): 6.5 m; distance between the center of mass of the roof and the top of the wall ( $h_R$ ):

340 0.4 m; specific weight of the masonry ( $P_m$ ): 19 kN/m<sup>3</sup>; specific weight of the reinforced  
 341 concrete ( $P_c$ ): 21 kN/m<sup>3</sup>; floor weight ( $P_f$ ): 4 kN/m<sup>2</sup>; friction coefficient roof – wall ( $\mu$ ): 0.4;  
 342 friction coefficient floor – wall ( $\mu$ ): 0.5; PGA for a return period of 475 years ( $a_g$ ): 2.538  
 343 m/s<sup>2</sup>;  $S_s$ : 1 (rock soil);  $S_i$ : 1 (flat area).



344  
 345 Figure 10. View of the building used as case study before and after the earthquake.

346  
 347 *4.2.1 Amatrice results*

348 The results obtained using the linear kinematic analysis are summarized in Table 3:

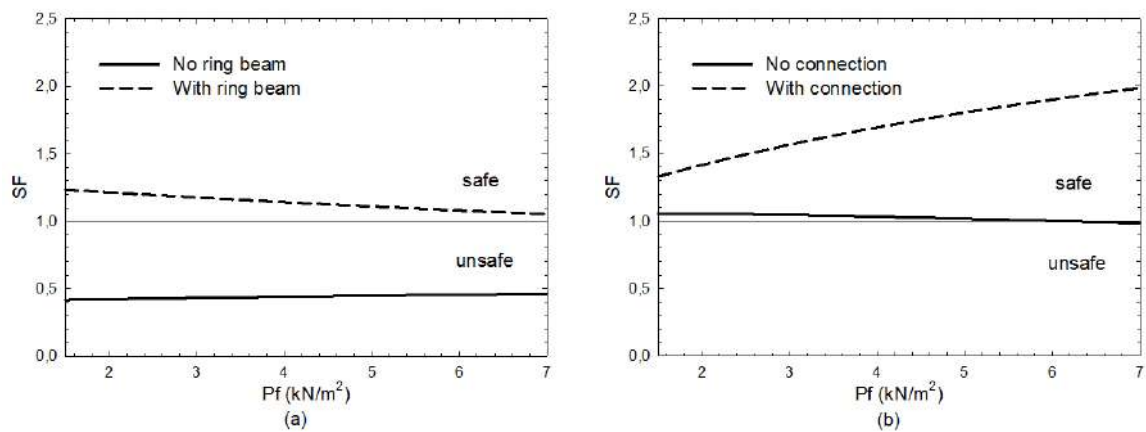
349  
 350 Table 3. Collapse load multipliers and safety factors for the Amatrice case study.

	2-storey overturning without ring beam	2-storey overturning with ring beam	2-storey vertical flexural behaviour without connection between floor and walls	2-storey vertical flexural behaviour with connection between floor and walls
$\alpha_C$	0.06	0.16	0.16	0.27
$SF$	0.44	1.14	1.03	1.70

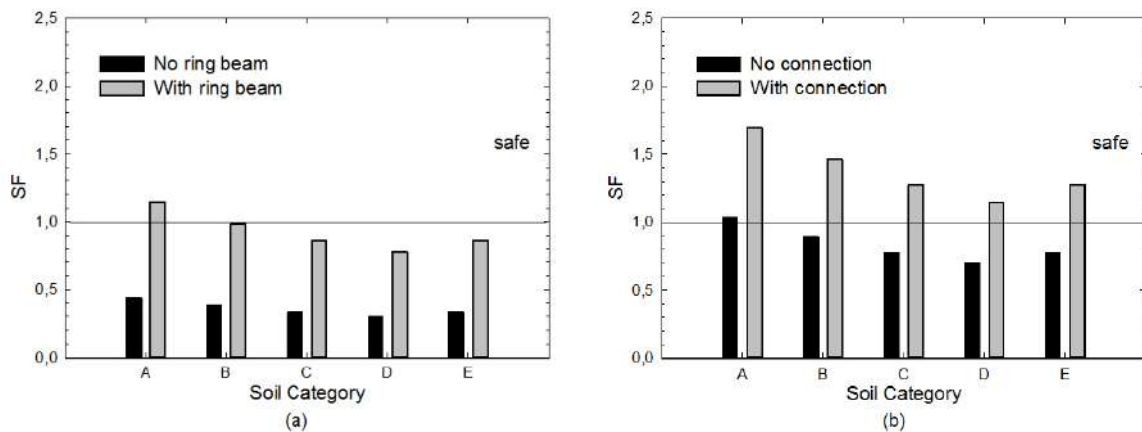
351  
 352 Comparing these results, it is clear that the configuration of overturning with no ring beam is  
 353 the less safe and the most probable. The presence of a ring beam increases the collapse load  
 354 multiplier of about 2.7 times for the overturning mechanism. On the other hand, the model  
 355 with connection at the top of the walls and at floor level is the safest and less probable case.  
 356 For the vertical flexural behaviour, the case with connection between floor and walls has 1.7  
 357 times as high of a collapse load as the case without connection has. Finally, it is possible to  
 358 observe that the mechanisms of overturning with ring beam and vertical flexural behaviour  
 359 without connection at floor level are almost equivalent.

360 Also for this case study, sensitivity analyses were performed for all parameters. The trends of  
 361 variation of other parameters are really similar to the previous ones, thus the considerations  
 362 done for the 1-storey model are still valid. The substantial difference between 2-storey  
 363 overturning and vertical flexural behaviour is that in the second case the safety factors are  
 364 higher. Omitting obvious and well-known results, it is worth to comment what happens when  
 365 the floor weight is changing (Figure 11). In both cases of overturning and in the case of

366 vertical flexural behaviour without connection, when the floor weight varies the safety factor  
 367 is not subject to significant changes. A slight reduction of SF can be observed in the  
 368 overturning scenario for the model with ring beam as the floor weight increases. A heavier  
 369 floor leads to greater horizontal inertial forces which contribute to the overturning. Instead,  
 370 for the mechanism of vertical flexural behaviour with connection, a heavy floor has a positive  
 371 impact since the stabilizing force increases. As far as the variation of soil category is  
 372 concerned, the values of the  $S_s$  coefficient that were used in the previous case study are still  
 373 valid (Table 2). It is interesting to notice that if the category of soil was not “A” (rock soil),  
 374 then only the mechanism of vertical flexural behaviour with connection would be safe  
 375 (Figure 12).



376  
 377 Figure 11. Floor weight vs. safety factor for the (a) overturning mechanism and the (b)  
 378 vertical flexural behaviour.



380  
 381 Figure 12. Soil category vs. safety factor for the (a) overturning mechanism and the (b)  
 382 vertical flexural behaviour mechanism.

383

### 384 5. Nonlinear kinematic analysis

385 Nonlinear kinematic analyses were carried out with the aim of supporting the results obtained  
 386 from linear analyses. The whole procedure follows the method proposed by Italian codes [5,



387 6], which is presented hereafter just in its main steps. The underlying idea of the method is to  
 388 determine the trend of the horizontal action that the structure is progressively able to  
 389 withstand during the collapse mechanism's evolution. This can be seen as the capacity curve  
 390 of an equivalent single degree of freedom system. The ultimate displacement capacity of the  
 391 local mechanism is then defined and compared with the seismic demand. Similarly to the  
 392 linear case, a multiplier  $\alpha$  is introduced and defined as the ratio between the applied  
 393 horizontal forces and the displacement  $d_k$  of a control point. The horizontal multiplier of  
 394 loads is evaluated at various configurations of the kinematic chain until reaching the collapse  
 395 condition, which is identified by a null multiplier  $\alpha$ , and a displacement  $d_{k,0}$ . Assuming that  
 396 involved actions (i.e. weights, external and internal forces) are constant during the evolution  
 397 of the mechanism, the curve is almost linear. In this case, only the evaluation of the  
 398 displacement  $d_{k,0}$  is required, and the curve is described by Eq. (12):

$$399 \quad \alpha = \alpha_0(1 - d_k / d_{k,0}) \quad (12)$$

400 where  $\alpha_0$  denotes the value of the multiplier capable of activating the analysed mechanism.  
 401 The problem can be solved considering a configuration varied from the static condition and  
 402 calculating the induced finite rotation  $\theta_k$  by means of virtual work principle. Reaching the  
 403 collapse situation, the overturning moment equals the stabilizing moment, and the resulting  
 404 nonlinear equation gives the final rotation  $\theta_{k,0}$ . Once the latter is determined, the  
 405 corresponding displacement  $d_{k,0}$  can be obtained. Let the control point be the center of gravity  
 406 of vertical forces, and  $h_{bar}$  be its distance from the base hinge. Eq. (13) expresses the relation  
 407 between the rotation angle and the displacement of the control point related to ultimate  
 408 capacity towards horizontal actions.

$$409 \quad d_{k,0} = h_{bar} \sin \theta_{k,0} \quad (13)$$

410 At this point, it is possible to define the  $\alpha - d_k$  curve according to Eq. (12). The equivalent  
 411 capacity curve should now be determined. It describes the relation between the acceleration  
 412  $a^*$  that activates the mechanism and displacement  $d^*$ . The first is obtained through Eq. (2) as  
 413 in the linear case, whereas  $d^*$  is given by Eq. (14).

$$414 \quad d^* = d_{k,0} \frac{\sum_{i=1}^{n+m} P_i \delta_{x,i}^2}{\delta_{x,k} \sum_{i=1}^{n+m} P_i \delta_{x,i}} \quad (14)$$

415 where:  $n+m$  is the number of weight forces that generates horizontal forces upon the macro-  
 416 elements;  $P_i$  is the generic weight force;  $\delta_{x,i}$  is the virtual horizontal displacement of the  
 417 application point of  $P_i$ ;  $\delta_{x,k}$  is the horizontal virtual displacement of the control point.

418 Making the same assumption done for the  $\alpha - d_k$  curve, the capacity curve can be derived from  
 419 Eq. (15).

$$420 \quad a^* = a_0^*(1 - d^* / d_0^*) \quad (15)$$

421 where  $d_0^*$  is the equivalent displacement corresponding to  $d_{k,0}$ .

422 The verification for the life safety limit state consists in a comparison between the ultimate  
 423 displacement capacity  $d_u^*$  of the local mechanism and the spectral displacement evaluated at  
 424 the period  $T_s$  (Eq. (16)):

$$425 \quad T_s = 2\pi \sqrt{\frac{d_s^*}{a_s^*}} \quad (16)$$

426 where  $a_s^*$ , is the acceleration correspondent to the displacement  $d_s^*$ , which is equal to  $0.4d_u^*$ ,  
 427 and  $d_u^* = 0.4d_0^*$ . Therefore, if  $d_u^*$  is greater than the spectral displacement  $S_{De}(T_s)$ , the  
 428 verification is fulfilled (Eq. (17)).

$$429 \quad SF = \frac{d_u^*}{S_{De}(T_s)} \geq 1 \quad (17)$$

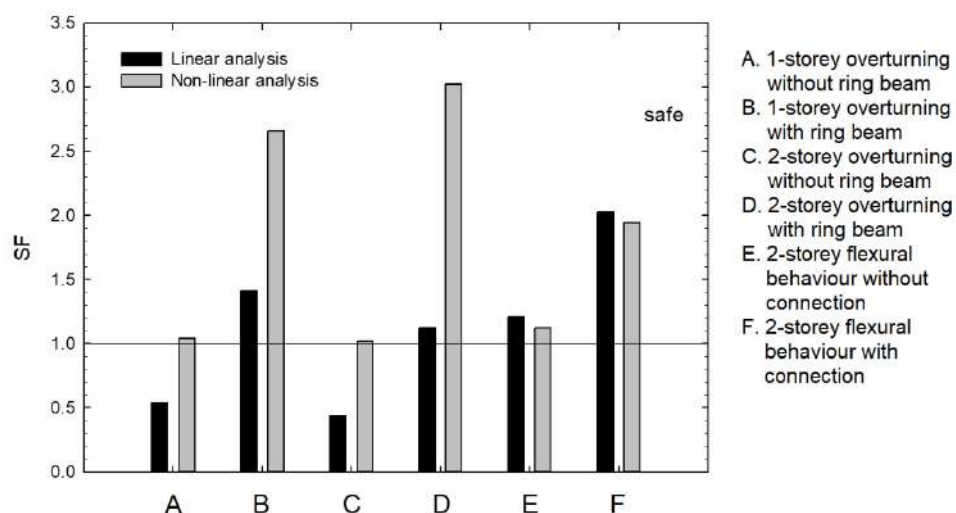
430 Table 4 shows obtained results for all analysed models. As expected, a lack of connection is  
 431 responsible of a small safety factor, always around 1 for the three studied cases. On the other  
 432 hand, the presence of a ring beam or floor-wall connections ensures much more capacity to  
 433 withstand larger ultimate displacements, which also means a higher safety level. The  
 434 difference is less exaggerated in the case of vertical flexural behaviour since the connection  
 435 between the floor and the wall makes the structure more rigid.

436 Comparing the linear with the nonlinear kinematic analysis in terms of safety factors, the bar  
 437 chart of Figure 13 can be plotted. The nonlinear kinematic analysis usually provides safety  
 438 coefficients that are two times or more the coefficient obtained with the linear analysis. This  
 439 confirms that a fast and preliminary analysis, such as the linear one, provides precautionary  
 440 results and it is recommended to understand if further investigations are needed. The  
 441 described trend is inverted in the cases of vertical flexural behaviour, although the nonlinear  
 442 safety factors are just slightly lower than linear ones. This phenomenon is due to the fact that  
 443 the weight of a reinforced concrete roof has a particularly positive effect for these two  
 444 models. In addition, the same analyses were repeated several times increasing the weight of  
 445 the roof for each iteration. In all cases the safety factor increased, but the increment in the  
 446 linear analysis was greater than in the nonlinear one.

447 Table 4. Results of the nonlinear kinematic analysis.

	Pescara del Tronto		Amatrice			
	1-storey overturning without ring beam	1-storey overturning with ring beam	2-storey overturning without ring beam	2-storey overturning with ring beam	2-storey flexural behaviour without connection	2-storey flexural behaviour with connection
$d_u^*$ [m]	0.089	0.227	0.093	0.326	0.041	0.074
$SF$	1.04	2.66	1.02	3.02	1.12	1.95

448



449  
 450 Figure 13. Comparison between safety factors resulting from linear and non-linear analyses.  
 451

452 **6. Conclusions**

453 The 2016 Central Italy earthquake caused damages and collapses of many masonry buildings,  
 454 including those retrofitted with reinforced concrete roofs. This type of retrofit intervention  
 455 seems to facilitate some collapse mechanisms if not properly executed. The paper presents a  
 456 simplified procedure to evaluate the seismic performance of masonry buildings retrofitted  
 457 with reinforced concrete roofs based on the linear kinematic analysis. Despite the analysis  
 458 method is well known, the proposed models have the advantage of explicitly considering the  
 459 interaction between the roof and the walls. Moreover, they require only few input parameters  
 460 that can be easily obtainable. The collapse load multiplier obtained as output of the linear  
 461 kinematic analysis was used to define a safety factor to have an idea whether a structure can  
 462 be considered safe towards a certain collapse mechanism.

463 The introduced analytical models are based on the overturning and vertical flexural behaviour  
 464 collapse mechanisms. In particular, the overturning scenario was analysed both for a 1-storey  
 465 and a 2-storey building, while the vertical flexural behaviour was considered for a 2-storey  
 466 building. Each scenario is studied twice: one configuration assuming that there is no  
 467 connection among the involved macro-elements and another one that provides for an  
 468 effective connection. The resulting six models were applied to two case studies, a 1-storey  
 469 and a 2-storey building both collapsed during the 2016 Central Italy earthquake. Results  
 470 highlight the importance of an efficient connection between the reinforced concrete roof and  
 471 masonry walls and that some configurations are unsafe, which means additional  
 472 investigations and possibly retrofit intervention are required. To account for the uncertainties  
 473 introduced by the simplified models, sensitivity analyses were performed. These allowed to  
 474 evaluate the influence of each input parameter to the overall safety level of the structure,  
 475 highlighting peculiar aspects in each mechanism. Nonlinear kinematic analyses were also  
 476 carried out and results were compared to those obtained from linear analyses. It was possible  
 477 to observe that the linear analysis is faster and more precautionary as it provides smaller  
 478 safety factors with respect to the nonlinear one.

479 Overall, the proposed analytical models represent an effective yet simple tool that can serve  
480 as a preliminary evaluation of the safety level of masonry structures retrofitted with  
481 reinforced concrete roofs. The method is not meant to be an alternative to other more refined  
482 analyses, such as finite element methods, that would allow for a more accurate safety  
483 verification. However, due to its simplicity, the procedure could be recommended when only  
484 few input data are available and be applied even by non-professional users to understand if  
485 further investigations and/or retrofit interventions are needed.

486

## 487 **Acknowledgement**

488 The research leading to these results has received funding from the European Research Council  
489 under the Grant Agreement n. ERC\_IDEAL RESCUE\_637842 of the project IDEAL  
490 RESCUE\_Integrated Design and Control of Sustainable Communities during Emergencies.

491

## 492 **References**

- 493 [1] “DM 16-01-1996. Norme tecniche per le costruzioni in zone sismiche”. 1996.  
494 Ministero dei Lavori Pubblici: Gazzetta Ufficiale.
- 495 [2] Calderini, C. 2008. “Use of reinforced concrete in preservation of historic buildings:  
496 conceptions and misconceptions in the early 20th century”. *International Journal of*  
497 *Architectural Heritage*, 2(1): 25-59.
- 498 [3] Dolce, M., A. Masi, and A. Goretti. 1999. *Damage to buildings due to 1997 Umbria-*  
499 *Marche earthquake*. Seismic Damage to Masonry Buildings, ed. A. Bernardini.  
500 Leiden: A a Balkema Publishers. 71-80.
- 501 [4] Donati, S., F. Marra, and A. Rovelli. 2001. “Damage and ground shaking in the town  
502 of Nocera Umbra during Umbria-Marche, central Italy, earthquakes: The special  
503 effect of a fault zone”. *Bulletin of the Seismological Society of America*, 91(3): 511-  
504 519.
- 505 [5] “DM 14-01-2008. Norme tecniche per le costruzioni”. 2008. Ministero dei Lavori  
506 Pubblici: Gazzetta Ufficiale.
- 507 [6] “Circolare 2 febbraio 2009, n. 617 Istruzioni per l'applicazione delle «Nuove norme  
508 tecniche per le costruzioni»”. 2009. Ministero delle Infrastrutture e dei Trasporti.
- 509 [7] Chen, Z.X., et al. 2016. “Nonlinear Analysis of Masonry Buildings Under Seismic  
510 Actions with a Multifan Finite Element”. *International Journal of Structural Stability*  
511 *and Dynamics*, 16(1).
- 512 [8] Valente, M. and G. Milani. 2016. “Non-linear dynamic and static analyses on eight  
513 historical masonry towers in the North-East of Italy”. *Engineering Structures*, 114:  
514 241-270.
- 515 [9] Milani, G. 2011. “Simple lower bound limit analysis homogenization model for in-  
516 and out-of-plane loaded masonry walls”. *Construction and Building Materials*,  
517 25(12): 4426-4443.
- 518 [10] Milani, G. and M. Valente. 2015. “Comparative pushover and limit analyses on seven  
519 masonry churches damaged by the 2012 Emilia-Romagna (Italy) seismic events:  
520 Possibilities of non-linear finite elements compared with pre-assigned failure  
521 mechanisms”. *Engineering Failure Analysis*, 47: 129-161.

- 522 [11] Arcidiacono, V., G.P. Cimellaro, and J.A. Ochsendorf. 2015. "Analysis of the failure  
523 mechanisms of the basilica of Santa Maria di Collemaggio during 2009 L'Aquila  
524 earthquake". *Engineering Structures*, 99: 502-516.
- 525 [12] Arcidiacono, V., et al. 2016. "The Dynamic Behavior of the Basilica of San Francesco  
526 in Assisi Using Simplified Analytical Models". *International Journal of Architectural  
527 Heritage*, 10(7): 938-953.
- 528 [13] Casapulla, C. and A. Maione. 2011. "Out-of-plane local mechanisms in masonry  
529 buildings. the role of the orientation of horizontal floor diaphragms". *Proceedings of  
530 the 9th Australasian Masonry Conference*: 225-235.
- 531 [14] Costa, A.A., et al. 2012. "Out-of-plane behaviour of existing stone masonry buildings:  
532 experimental evaluation". *Bulletin of Earthquake Engineering*, 10(1): 93-111.
- 533 [15] Guadagnuolo, M., A. Donadio, and G. Faella. 2012. *Out-of-plane failure mechanism  
534 of masonry building corners*. Structural Analysis of Historical Constructions, Vols 1-  
535 3., ed. J. Jasienko. Structural Analysis of Historical Constructions, Vols 1-3. 481-488.
- 536 [16] Makris, N. 2014. "The role of the rotational inertia on the seismic resistance of  
537 free-standing rocking columns and articulated frames". *Bulletin of the Seismological  
538 Society of America*, 104(5): 2226-2239.
- 539 [17] Makris, N. and M.F. Vassiliou. 2014. "Dynamics of the rocking frame with vertical  
540 restrainers". *Journal of Structural Engineering*, 141(10): 04014245.
- 541 [18] Giresini, L., M. Fragiocomo, and M. Sassu. 2016. "Rocking analysis of masonry walls  
542 interacting with roofs". *Engineering Structures*, 116: 107-120.
- 543 [19] Borri, A., G. Castori, and A. Grazini. 2009. "Retrofitting of masonry building with  
544 reinforced masonry ring-beam". *Construction and Building Materials*, 23(5): 1892-  
545 1901.
- 546 [20] Guadagnuolo, M. and G. Faella. 2015. "Floor masonry beams reinforced by BFRG  
547 Innovation on advanced composite materials for strengthening of masonry structures",  
548 in *XIII Forum Internazionale di Studi "Le Vie dei Mercanti"–HERITAGE and  
549 TECHNOLOGY MIND KNOWLEDGE EXPERIENCE*. La scuola di Pitagora editrice,  
550 pp. 2108-2115.
- 551 [21] Fayala, I., O. Limam, and I. Stefanou. 2016. "Experimental and numerical analysis of  
552 reinforced stone block masonry beams using GFRP reinforcement". *Composite  
553 Structures*, 152: 994-1006.
- 554 [22] Derakhshan, H., et al. 2014. "In situ out-of-plane testing of as-built and retrofitted  
555 unreinforced masonry walls". *Journal of Structural Engineering*, 140(6): 04014022.
- 556 [23] Boscato, G., et al. 2014. "Seismic Behavior of a Complex Historical Church in  
557 L'Aquila". *International Journal of Architectural Heritage*, 8(5): 718-757.
- 558 [24] Casapulla, C. and L.U. Argiento. 2016. "The comparative role of friction in local out-  
559 of-plane mechanisms of masonry buildings. Pushover analysis and experimental  
560 investigation". *Engineering Structures*, 126: 158-173.
- 561

## **Highlights**

- The paper presents a preliminary simplified procedure to evaluate the seismic safety of masonry buildings retrofitted with reinforced concrete roofs.
- Effective connection between RC roof and walls is crucial to be in a safe condition
- Sensitivity analyses performed to evaluate the influence of each input parameter
- In most cases nonlinear kinematic analyses provide larger safety factors

# The role of reinforced concrete roofs in the seismic performance of masonry buildings

Alessandro Cardoni<sup>a</sup>, Gian Paolo Cimellaro<sup>b,\*</sup>

<sup>a</sup>PhD Student, Department of Structural, Geotechnical and Building Engineering, Politecnico di Torino, Corso Duca degli Abruzzi 24, 10129, Turin, Italy. E-mail: [alessandro.cardoni@polito.it](mailto:alessandro.cardoni@polito.it)

<sup>b</sup>Associate Professor, Department of Structural, Geotechnical and Building Engineering, Politecnico di Torino, Corso Duca degli Abruzzi 24, 10129, Turin, Italy. E-mail: [gianpaolo.cimellaro@polito.it](mailto:gianpaolo.cimellaro@polito.it)

\*Corresponding author. Tel.: +39 011 0904801. E-mail: [gianpaolo.cimellaro@polito.it](mailto:gianpaolo.cimellaro@polito.it)

## Abstract

The 2016 Central Italy earthquake caused many collapses of existing masonry buildings that had previously been retrofitted with reinforced concrete roofs. The aim of this paper is to explore the role of these roofs in the seismic behaviour of masonry buildings. Simple analytical models are presented to illustrate two typical out-of-plane collapse mechanisms: wall overturning and vertical flexure. The models are based on linear kinematic analysis, which allows fast modelling and calculation of a coefficient that can be used to assess the safety level of a structure. Nonlinear kinematic analyses were also performed. Both methods were applied to two case studies taken from areas struck by the earthquake. Results show that linear analysis represents an effective tool for preliminary verifications that can allow one to understand whether retrofit interventions are needed.

Keywords: masonry, reinforced concrete roof, collapse, retrofit, kinematic analysis, Central Italy earthquake

## 1. Introduction

After the 24<sup>th</sup> August 2016 Central Italy earthquake, most of the buildings of small towns nearby the epicenter were declared unsafe and several structures collapsed completely. Poor material quality and scant building techniques were certainly the main reason of collapses. However, inadequate retrofit interventions also contributed to the disruptive effect of the seismic event. For instance, the replacement of the old wooden roofs with reinforced concrete roofs seemed to facilitate some mechanisms that led to severe damages and collapses. This type of retrofitting was broadly adopted in the 80s and 90s since it was believed to be effective against seismic actions. In fact, it was the Italian code itself to recommend it [1]. Moreover, at that period there was a massive use of concrete that led to a gradual abandon of research and experimental tests on masonry [2]. The overall idea was to put robust structures such as RC roofs and floors connected to perimetric walls by means of RC ring beams to avoid independent movements of masonry macro-elements. After Tolmezzo earthquake in 1976, this and other retrofitting techniques became part of technical codes, until Umbria and Marche earthquake in 1997 [3, 4].



60  
61  
62  
63 40 This event pointed out the disadvantages of heavy and stiff roofs and floors. In fact, if vertical  
64 41 structures are not robust enough, they are indeed the primary cause of collapses. The significant  
65 42 stiffness and load increment at the top have led to the collapse of the walls, which were made of  
66 43 poor materials and not strengthened. Conversely, there were also many cases of masonry  
67 44 structures retrofitted with reinforced concrete roofs that withstood the earthquake with no  
68 45 significant damages (Figure 1).



46  
47 Figure 1. Masonry buildings retrofitted with concrete roof not collapsed after the earthquake in  
48 Pescara del Tronto (a-b) and small villages near Accumoli (c-d).

50 However, there is no guarantee that those buildings are safe. Therefore, in this paper a simple  
51 verification procedure that is able to estimate the level of safety of masonry buildings with  
52 reinforced concrete roofs is implemented. The adopted approach is based on the linear kinematic  
53 analysis, which is also described by Italian codes [5, 6]. Despite the method is well known in its  
54 theoretical formulation, it is rarely used and usually the effect of the roof and the connection  
55 among structural elements are neglected. This research contributes to the current literature with  
56 practical applications of the kinematic analysis introducing simplified analytical models that  
57 take into account the effect of reinforced concrete roofs. An additional advantage of the  
58 proposed models is that the number of input parameters has been reduced as much as possible so  
59 that the analysis does not require any particular investigation or survey to be carried out. A  
60 safety factor was also defined to assess the safety level of the building towards different collapse



119  
120  
121 61 mechanisms. The choice of a simplified procedure has been made in order to have a fast tool  
122 62 which could be used even by non-professional users. The method would allow property owners  
123 63 to understand if they are in danger. For instance, if the obtained safety factor is low or close to  
124 64 the unsafe threshold, further investigations should be conducted. More detailed methods have  
125 65 been studied by many authors to describe masonry buildings behaviour, but they need to be  
126 66 calibrated and the input data are often not accessible [7-10]. Obviously, results will not be as  
127 67 accurate, and a certain margin of error should be taken into account in final considerations.  
128 68 Nonetheless, they can provide relevant preliminary information about the structure. In addition,  
129 69 in the literature there is a number of studies about masonry where analytical models turned out  
130 70 to be highly effective and close to the real behaviour [11, 12].

133 71 After defining the formulation, the method is applied to different models describing the  
134 72 overturning and the vertical flexural behaviour. The models derive from those commonly used  
135 73 to study the out-of-plane mechanisms [13-15] and the arch rocking [16-18]. To analyse the  
136 74 influence of the connection between the roof and the floor to the walls, a ring beam is also  
137 75 considered. The presence of a reinforced concrete (RC) ring beam is dangerous if it is not well  
138 76 connected to masonry walls and if the latter is not strengthened. Furthermore, the spread of  
139 77 reinforced concrete in the construction sector, led to wrong applications in the interventions of  
140 78 existing buildings. Nowadays there are many solutions to realize effective structural  
141 79 connections, such as reinforced masonry ring beams [19]. The use of innovative composite  
142 80 materials has become a common practice in retrofit strategies. Several studies have been carried  
143 81 out in this field which has allowed to investigate the behavior of strengthened beams [20, 21]  
144 82 and strengthened masonry walls through out-of-plane tests [22].

148 83 Two case studies taken from two towns struck by the abovementioned earthquake were  
149 84 analyzed, but the method can be extended to any building by choosing appropriate parameters.  
150 85 Both examples were selected by considering typical houses in the area, built with local materials  
151 86 and poor construction techniques and retrofitted with reinforced concrete roofs. The first one is  
152 87 1-storey building while the second one has two storeys and thus also the action of the inter-  
153 88 storey floor is considered in the model. For each model, the linear kinematic analysis is repeated  
154 89 for different values of the input parameters, as they could be affected by uncertainty. In this way  
155 90 it is possible to see the influence of a single parameter and what happens if it is over-estimated  
156 91 or under-estimated. Finally, nonlinear analyses are performed in order to compare the results and  
157 92 understand if the additional computational effort of a more refined method is worth it.

## 160 93 161 94 **2. The linear kinematic analysis**

163 95 In existing masonry buildings there are often collapses due to a loss of equilibrium of some  
164 96 portions of bearing structures. In general, these types of mechanisms happen when seismic  
165 97 forces act in the out-of-plane direction. The linear kinematic analysis can be used to study  
166 98 these phenomena and for the verification process. It is based on the choice of the possible  
167 99 mechanisms that are most likely to happen. These ones are assumed by evaluating the current  
168 100 cracking state and analyses performed on similar buildings. In the literature there are plenty  
169 101 of studies on historical buildings, such as churches, which are helpful to clarify how the  
170 102 collapse process activates and evolve [23]. The ability to detect the most probable  
171 103 mechanisms is crucial to prevent local or global collapses, since it is possible to run specific  
172 104 analyses and consequently suggest specific interventions.

178  
179  
180  
181 105 The linear kinematic approach schematizes the building in a discrete number of macro-  
182 106 elements which move according to their boundary conditions. For this reason, the  
183 107 assumptions are that the material has no tensile strength and infinite compressive strength. In  
184 108 each rigid block, vertical loads (including dead and external loads) and a system of horizontal  
185 109 forces are applied. Horizontal forces are proportional to the vertical loads through a  
186 110 coefficient called load multiplier ( $\alpha$ ). Incrementing the load multiplier, it is possible to  
187 111 evaluate the horizontal force that activates a specific mechanism.  $\alpha_C$  is named the collapse  
188 112 load multiplier, and it is calculated with the principle of virtual works. Therefore, the total  
189 113 work of the external forces ( $L_e$ ) has to be equal to the total work of the internal forces ( $L_i$ )  
190 114 which in this case is null as shown in Eq. (1):

$$191 \quad 114 \quad L_e = \alpha_C \left( \sum_{i=1}^n W_i \cdot \delta_{x,i} + \sum_{j=n+1}^{n+m} W_j \cdot \delta_{x,j} \right) - \sum_{i=1}^n W_i \cdot \delta_{y,i} - \sum_{h=1}^o F_h \cdot \delta_h = L_i = 0 \quad (1)$$

192  
193 115  
194  
195  
196 116 where:  $n$  is the number of the weight forces applied to all macro-elements;  $m$  is the number of  
197 117 weight forces that generate horizontal forces upon macro-elements;  $o$  is the number of  
198 118 external forces;  $W_i$  is the generic weight force;  $W_j$  is the generic weight force that generates  
199 119 horizontal forces upon macro-elements;  $\delta_{x,i}$  is the virtual horizontal displacement of the point  
200 120 where the  $i$ -th weight force is applied;  $\delta_{y,i}$  is the virtual vertical displacement of the point  
201 121 where the  $i$ -th weight force is applied;  $F_h$  is the generic external force;  $\delta_h$  is the virtual  
202 122 displacement of the point where the generic external force  $F_h$  is applied. Eq. (1) often  
203 123 becomes an equilibrium equation between a stabilizing moment and an overturning moment,  
204 124 so it is not necessary to calculate the virtual displacement. The method is also used to  
205 125 determine the most probable collapse mechanism which is the one that requires less energy to  
206 126 be activated (i.e. the one with the lower load multiplier). However, the decay conditions of  
207 127 masonry should never be neglected since they are able to reveal if a specific mechanism has  
208 128 already been activated. Once  $\alpha_C$  is calculated, it is possible to obtain the acceleration that  
209 129 generates the mechanism (Eq. (2)).

$$210 \quad 128 \quad a_0^* = \frac{\alpha_C \cdot \sum_{i=1}^{n+m} P_i}{M^* \cdot FC} \quad (2)$$

211 129  
212  
213  
214 130  
215  
216  
217 131 where  $FC$  is a coefficient that depends on the level of knowledge about the masonry  
218 132 structure. The level of knowledge is based on information like geometry, construction details,  
219 133 and material properties. Such data can be acquired in different ways, from generic research  
220 134 and visual inspection to extensive tests and measurements. Since the material strength is not  
221 135 considered in this research, only basic information about geometric characteristics, type of  
222 136 masonry panels and construction details was collected. According to the Italian code [6],  
223 137 three level of knowledge can be identified: limited, extended and exhaustive. Due to the  
224 138 limited available data, the level of knowledge is limited. In this case, the code reports the  $FC$   
225 139 coefficient has to be assumed equal to 1,35 which reduces the acceleration that generates the  
226 140 mechanism.  $M^*$  is the participating mass, calculated considering the virtual displacements of  
227 141 the points where the loads are applied, as shown in Eq. (3) [6]:

$$M^* = \frac{\left( \sum_{i=1}^{n+m} P_i \cdot \delta_{x,i} \right)^2}{g \cdot \sum_{i=1}^{n+m} P_i \cdot \delta_{x,i}^2} \quad (3)$$

The acceleration given by Eq. (2) has now to be compared with an allowable acceleration. This one is given by Eq. (4), which is valid when the analysed blocks are in contact with the ground, meaning that the mechanism involves ground floor walls:

$$a^* = \frac{a_g \cdot S}{q} \quad (4)$$

where:  $a_g$  is the peak ground acceleration at the site determined, as indicated by Italian codes, for a return period of 475 years;  $q$  is the reduction factor which can be assumed equal to 2 for regular masonry structures;  $S$  is given by the product of two coefficients:  $S_s$  that depends on the soil category and represents the stratigraphic amplification, and  $S_t$  which takes into account the effects of the topographical amplification and depends on the surface configuration of the soil.

It is clear that the acceleration that activates the mechanism should be greater than the allowable one. To quickly verify this, it is possible to introduce a safety factor which is the ratio between the two accelerations (Eq. (5)):

$$SF = \frac{a_0^*}{a^*} \geq 1 \quad (5)$$

### 3. Analytical models

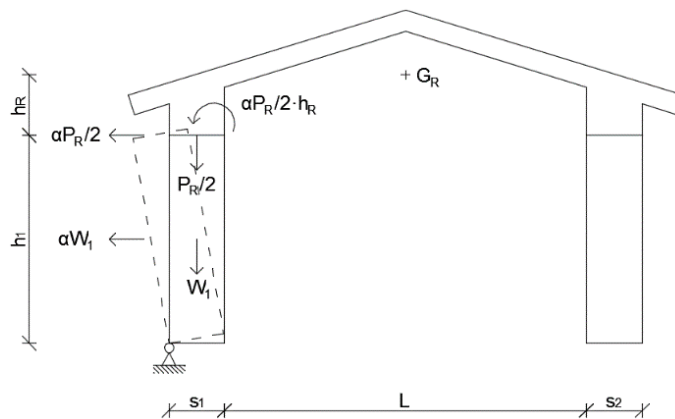
In some cases, there are mechanisms that are suggested by the building itself just looking to the geometry, the nature of the structural elements, the cracking state, the interventions occurred over the years, etc. The linear kinematic analysis is a powerful tool that can be used to describe local mechanisms that have been observed after disruptive earthquakes. If only out-of-plane mechanisms are considered, then they can be basically grouped in three categories: (i) overturning, (ii) vertical flexural behaviour and (iii) horizontal flexural behaviour. In this paper only the first two categories are considered since they were the main cause of collapses during the Central Italy earthquake. In addition, for these two mechanisms the presence of a reinforced concrete roof is more crucial. For the overturning, two cases were studied, a 1-storey and a 2-storey building, whereas for the vertical flexural behaviour only the 2-storey building was studied, taking into account also the effect of the inter-storey. The considered macro-elements are the walls, the floor, and the reinforced concrete roof. This one is assumed as an element that transfers only vertical loads to the walls and no lateral thrusts. Therefore, it is modelled as a rigid block with a large mass. The effects of perpendicular walls are neglected, as in many real cases there are no connections. All models consider alternatively the presence and the absence of connections between roof and walls (by means of a ring beam) and between floor and walls. When there is a ring beam the roof is fixed to the walls and moves with them, while when there is no connection the roof is considered simply supported.

296  
297  
298  
299  
300  
301  
302  
303  
304  
305  
306  
307  
308  
309  
310  
311  
312  
313  
314  
315  
316  
317  
318  
319  
320  
321  
322  
323  
324  
325  
326  
327  
328  
329  
330  
331  
332  
333  
334  
335  
336  
337  
338  
339  
340  
341  
342  
343  
344  
345  
346  
347  
348  
349  
350  
351  
352  
353  
354

178

179 **3.1 1-storey overturning without ring beam**

180 This is the case of simple overturning where there is no ring beam, and therefore no  
181 connection between the top of the wall and the roof. For this reason, the macro-elements are  
182 independent one from another and only one wall is subjected to overturning. Figure 2  
183 illustrates the mechanism and the forces involved.  $W_l$  is the weight of the left wall,  $P_R$  is the  
184 weight of the roof applied in its center of mass  $G_R$  and split equally between the two walls.



185

186 Figure 2. Calculating scheme for 1-storey overturning without ring beam.

187

188 According to Eq. (1) the load multiplier that leads to collapse for this configuration is given  
189 by Eq. (6):

190

$$\alpha_C = \frac{W_l \cdot \frac{s_l}{2} + \frac{P_R}{2} \cdot \frac{s_l}{2}}{W_l \cdot \frac{h_l}{2} + \frac{P_R}{2} \cdot (h_l + h_r)} \quad (6)$$

191 where  $s_l$  is the thickness of left wall;  $h_l$  is the height of walls;  $h_r$  is the distance between the  
192 top of walls and the center of mass ( $G_R$ ) of the roof, and  $L$  is the span length.

193

194 **3.2 1-storey overturning with ring beam**

195 If there is a ring beam the two external walls are connected at the top to realize the so called  
196 “box-like” behaviour. Macro-elements are no more independent, so they move together until  
197 the loss of equilibrium. As shown in Figure 3 both walls rotate around the hinge at the bottom  
198 under a seismic action. The effect of the ring beam is modelled using a force acting in the  
199 opposite direction of the kinematic movement. To a first approximation, it can be calculated  
200 as the product of the friction coefficient  $\mu$  and the weight of the roof  $P_R$ . For the estimation of  
201 the friction coefficient there are many experimental tests available in literature [24].  
202 However, since the proposed model is simplified and no detailed information about the  
203 materials were available, the guidelines provided by national codes were followed [5, 6]. In  
204 particular, as a precautionary measure, a friction coefficient of 0.4 was used, which is the  
205 lowest among the suggested values.





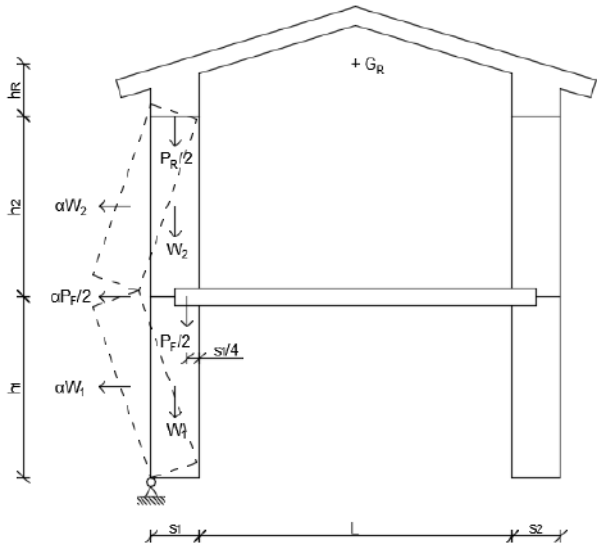
473  
474  
475  
476  
477  
478  
479  
480  
481  
482  
483  
484  
485  
486  
487  
488  
489  
490  
491  
492  
493  
494  
495  
496  
497  
498  
499  
500  
501  
502  
503  
504  
505  
506  
507  
508  
509  
510  
511  
512  
513  
514  
515  
516  
517  
518  
519  
520  
521  
522  
523  
524  
525  
526  
527  
528  
529  
530  
531

238

239 **3.5 2-storey flexural behaviour without connection between floor and walls**

240 Vertical flexural behaviour can occur in any part of the wall. It can be seen as a triple-hinged  
 241 arch where, in this specific case, the hinges are located at the bottom, at the top, and at the  
 242 inter-storey level. This means that the mechanism is activated by the horizontal inertial force  
 243 caused by the floor during the seismic action. The upper level wall is connected at the top of  
 244 the roof, whereas the inter-storey floor is not connected to the walls (Figure 6). The collapse  
 245 load multiplier  $\alpha_C$  is given by Eq. (10):

246 
$$\alpha_C = \frac{W_1 \cdot \frac{s_1}{2} + W_2 \cdot \left( s_1 + \frac{s_1}{2} \cdot \frac{h_1}{h_2} \right) + \frac{P_F}{2} \cdot \frac{3s_1}{4} + \frac{P_R}{2} \cdot \left( s_1 + \frac{s_1}{2} \cdot \frac{h_1}{h_2} \right)}{W_1 \cdot \frac{h_1}{2} + W_2 \cdot \left( h_1 \cdot \frac{h_1}{h_2} + \frac{h_2}{2} \cdot \frac{h_1}{h_2} \right) + \frac{P_F}{2} \cdot h_1} \quad (10)$$



247  
248 Figure 6. Calculating scheme for vertical flexural behaviour without floor-walls connection.

249

250 **3.6 2-storey flexural behaviour with connection between floor and walls**

251 In this model the floor is well connected to the walls so that it can pull them together, but  
 252 eventually it detaches. To represent this type of connection, a friction force proportional to  
 253 the floor weight is considered at the inter-storey level (Figure 7).

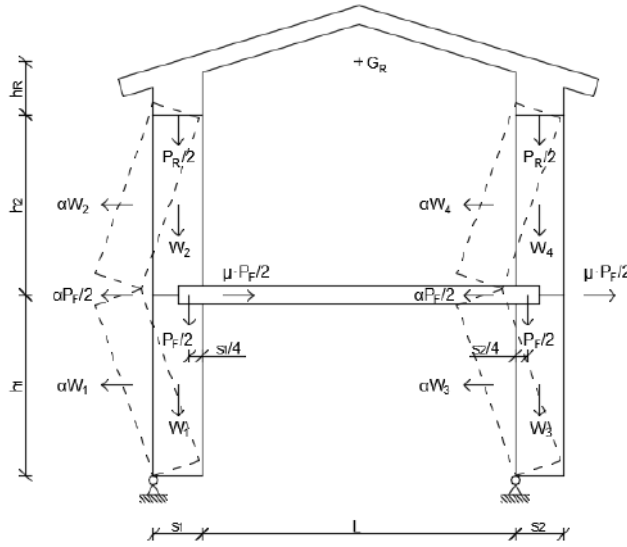


Figure 7. Calculating scheme for vertical flexural behaviour with floor-walls connection.

Eq. (11) allows to get the collapse load multiplier for this model:

$$\alpha_C = \frac{W_1 \cdot \frac{s_1}{2} + W_2 \cdot \left( s_1 + \frac{s_1}{2} \cdot \frac{h_1}{h_2} \right) + W_3 \cdot \frac{s_2}{2} + W_4 \cdot \left( s_2 + \frac{s_2}{2} \cdot \frac{h_1}{h_2} \right) + \frac{P_F}{2} \cdot \frac{3s_1}{4} + \frac{P_F}{2} \cdot \frac{s_2}{4}}{(W_1 + W_3) \cdot \frac{h_1}{2} + (W_2 + W_4) \cdot \left( h_1 \cdot \frac{h_1}{h_2} + \frac{h_2}{2} \cdot \frac{h_1}{h_2} \right) + P_F \cdot h_1} + \frac{\frac{P_R}{2} \cdot \left( s_1 + \frac{s_1}{2} \cdot \frac{h_1}{h_2} \right) + \frac{P_R}{2} \cdot \left( s_2 + \frac{s_2}{2} \cdot \frac{h_1}{h_2} \right) + (\mu \cdot P_F) \cdot h_1}{(W_1 + W_3) \cdot \frac{h_1}{2} + (W_2 + W_4) \cdot \left( h_1 \cdot \frac{h_1}{h_2} + \frac{h_2}{2} \cdot \frac{h_1}{h_2} \right) + P_F \cdot h}$$

## 4. Case studies

### 4.1 Pescara del Tronto case study

Figure 8 shows a house in Pescara del Tronto completely collapsed after the 2016 Central Italy earthquake, which can be used as an example to apply the 1-storey model. The data that were used as input in the model are the following: wall thickness ( $s = s_1 = s_2$ ) = 0.4 m; roof thickness ( $s_R$ ) = 0.15 m; wall height ( $h_1$ ) = 3 m; wall length ( $l_w$ ) = 7 m; span length ( $L$ ) = 5 m; distance between the center of mass of the roof and the top of the wall ( $h_R$ ) = 0.4 m; specific weight of masonry ( $P_m$ ) = 19 kN/m<sup>3</sup>; specific weight of reinforced concrete ( $P_c$ ) = 21 kN/m<sup>3</sup>; friction coefficient roof – wall ( $\mu$ ) = 0.4; PGA for a return period of 475 years ( $a_g$ ) = 2.489 m/s<sup>2</sup>;  $S_s$  = 1 (rock soil);  $S_t$  = 1.2 (top of a hill). The weight of the walls was calculated as  $W_i = h_i \cdot l_w \cdot s_i \cdot P_m$ , where  $i=1, 2$ , while the weight of the roof as

$$W_i = 2 \cdot \left[ \sqrt{(s + L/2)^2 + h_r^2} \cdot l_w \cdot s_r \cdot P_c \right].$$





Figure 8. View of the building used as case study before and after the earthquake.

As already mentioned, most of the data are geometrical so they can be easily collected. Only the PGA needs to be calculated referring to the information given by the Italian code [5]. In this case, the location is fixed, so the value can be determined analytically. The value used for  $S_s$  is referred to rock soil, while the one used for  $S_t$  is referred to the top of a hill as there is evidence of a slope behind the building.

#### 4.1.1 Pescara del Tronto results

The results using the linear kinematic analysis and verification are reported in Table 1.

Table 1. Collapse load multipliers and safety factors for the Pescara del Tronto case study.

	1-storey overturning without ring beam	1-storey overturning with ring beam
$\alpha_c$	0.10	0.26
$SF$	0.57	1.48

Comparing the load multipliers, it can be observed that the first mechanism is more likely to happen as the 1-storey overturning with ring beam case has a collapse load 2.6 times higher than the 1-storey overturning without ring beam. This is confirmed by the fact that the safety factor in the case without ring beam is lower and it is below the safety threshold. Indeed, as shown in Figure 8 there is no connection between roof and walls. If this kind of analysis was carried out in a pre-earthquake situation, it would have been possible to demonstrate how the building was unsafe towards a seismic event with a return period of 475 years. The actual demand of 2016 earthquake was larger than the one used as input for this verification procedure. However, the aim of the method is to report if retrofitting is needed to improve the level of safety. Validation analyses were not performed at this stage, but adequate interventions could have likely prevented the structure from a complete collapse.

A sensitivity analysis was carried out to assess the impact of the chosen input parameters on results. Most relevant outcomes were then plotted in graphs with the varying parameter on the  $x$  axis and the safety factor  $SF$  on the  $y$  axis. Figure 9(a) shows that when there is no

650  
651  
652  
653  
654  
655  
656  
657  
658  
659  
660  
661  
662  
663  
664  
665  
666  
667  
668  
669  
670  
671  
672  
673  
674  
675  
676  
677  
678  
679  
680  
681  
682  
683  
684  
685  
686  
687  
688  
689  
690  
691  
692  
693  
694  
695  
696  
697  
698  
699  
700  
701  
702  
703  
704  
705  
706  
707  
708

300 friction the two mechanisms are equivalent because of the symmetry of the systems and the  
 301 configuration is unsafe. The minimum friction coefficient to ensure a safety factor greater  
 302 than 1 is 0.2. As predictable, the impact of the friction is overall positive: it is enough to build  
 303 a ring beam able to ensure a friction coefficient of 0.4 and triple the safety factor. In Figure  
 304 9(b) the span length is varying, resulting in an increase or decrease in the weight of the roof.  
 305 This has almost no effects in the case without ring beam, which remains unsafe in the whole  
 306 range of variation. On the other hand, since the friction force is proportional to the weight of  
 307 the roof, increasing the span length leads to a significant increment of the safety factor. When  
 308 the masonry specific weight of the masonry varies, safety factor remains almost constant  
 309 (Figure 9(c)). The weight of the walls has indeed a twofold effect since it contributes to both  
 310 stabilizing and overturning forces. Also, looking at the equations that lead to determine SF (in  
 311 particular Eqs. (6-7) and Eq. (2)), it can be noticed how the weight appears always at both  
 312 nominator and denominator. Therefore, in the calculation steps its variation tends to have  
 313 negligible effects. Figure 9(d) shows the influence of the wall thickness. In the first case,  
 314 without ring beam, an increment of the wall thickness corresponds to a linear and  
 315 considerable increment of the *SF*. However, almost 70 cm walls are required to be in the safe  
 316 area. In the second case, there is an asymptotic trend. It means that for low thicknesses the  
 317 presence of the ring beam is effective (e.g. for  $s = 20$  cm the *SF* is two times the *SF* in the  
 318 case with no ring beam), but for high thicknesses the structure is so massive that the presence  
 319 of the ring beam at the top is irrelevant. Finally, in Figure 9(e) different soil categories are  
 320 taken into account by varying the abovementioned parameter  $S_s$ . Following the guidelines  
 321 provided by the Italian seismic codes, the possible values  $S_s$  can assume were calculated  
 322 (Table 2). A rock soil allows to have higher safety factors, whereas if the quality gets worse  
 323 there is a decreasing trend, except for category E (coarse soil upon a stiff or soft soil).

324  
325 Table 2. Values of the parameter  $S_s$  for different soil categories.

Soil category	Description	$S_s$
A	Rock soil ( $V_{s30} > 800$ m/s)	1.00
B	Soft rock and very dense soil ( $360 \text{ m/s} < V_{s30} < 800 \text{ m/s}$ )	1.16
C	Stiff soil ( $180 \text{ m/s} < V_{s30} < 360 \text{ m/s}$ )	1.33
D	Soft soil ( $V_{s30} < 180 \text{ m/s}$ )	1.48
E	Coarse soil upon stiff or soft soil	1.33

326  
327

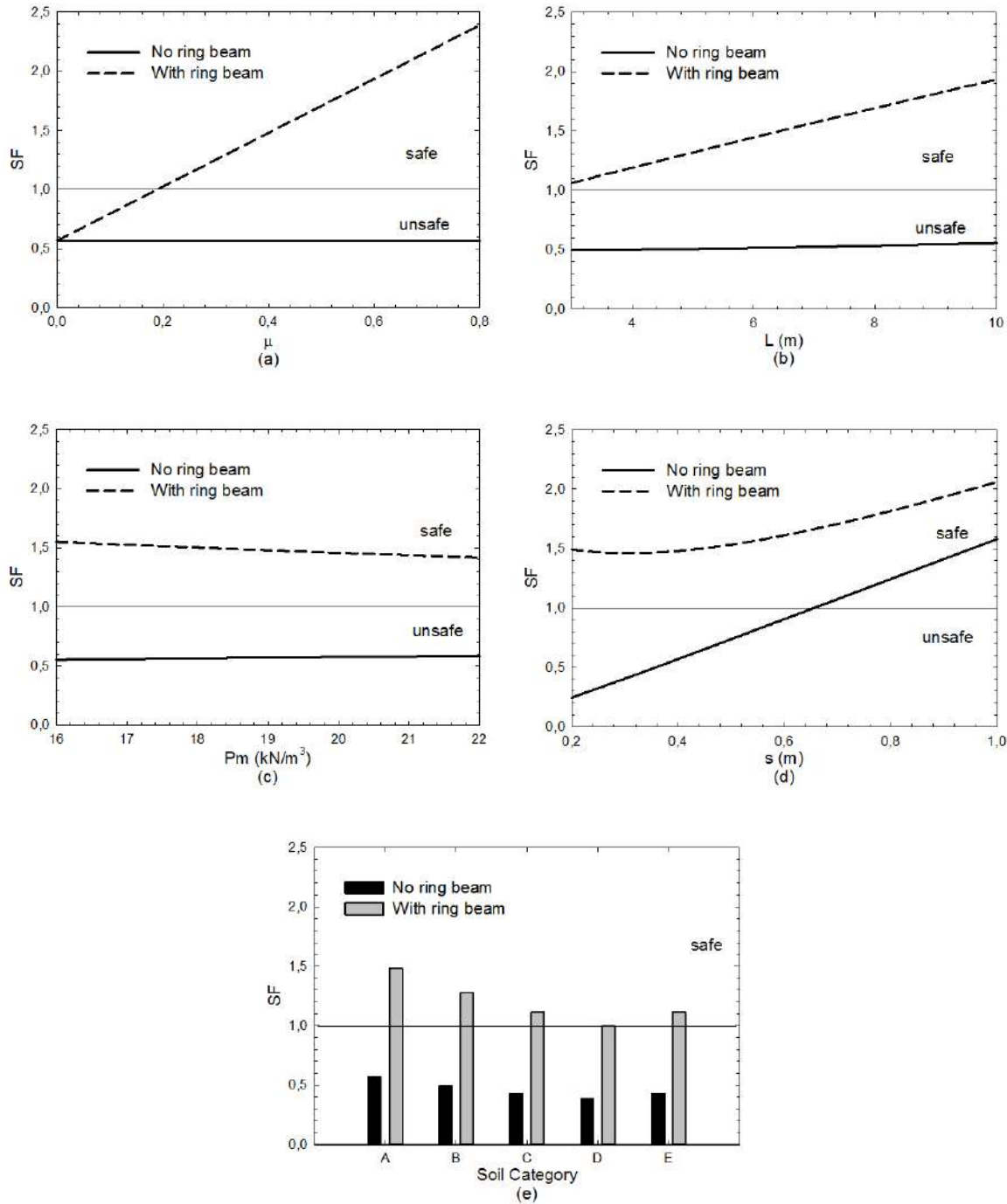


Figure 9. (a) Friction coefficient vs. safety factor, (b) span length vs. safety factor, (c) masonry specific weight vs. safety factor, (d) wall thickness vs. safety factor, (e) soil category vs. safety factor.

#### 4.2 Amatrice case study

The 2-floor models were tested through the building in Figure 10 which was located in Amatrice. The data used as input for the analysis are the following: wall thickness ( $s_1 = s_2$ ): 0.4 m; roof thickness ( $s_R$ ): 0.15 m; wall height ( $h_1 = h_2$ ): 3 m; wall length ( $l_w$ ): 11 m; span length ( $L$ ): 6.5 m; distance between the center of mass of the roof and the top of the wall ( $h_R$ ):

768  
 769  
 770 340 0.4 m; specific weight of the masonry ( $P_m$ ): 19 kN/m<sup>3</sup>; specific weight of the reinforced  
 771 341 concrete ( $P_c$ ): 21 kN/m<sup>3</sup>; floor weight ( $P_f$ ): 4 kN/m<sup>2</sup>; friction coefficient roof – wall ( $\mu$ ): 0.4;  
 772 342 friction coefficient floor – wall ( $\mu$ ): 0.5; PGA for a return period of 475 years ( $a_g$ ): 2.538  
 773 343 m/s<sup>2</sup>;  $S_s$ : 1 (rock soil);  $S_i$ : 1 (flat area).  
 775  
 776  
 777  
 778  
 779  
 780  
 781  
 782  
 783  
 784  
 785  
 786



787 345 Figure 10. View of the building used as case study before and after the earthquake.  
 788  
 789 346

790  
 791 347 *4.2.1 Amatrice results*

792 348 The results obtained using the linear kinematic analysis are summarized in Table 3:  
 793  
 794 349

796 350 Table 3. Collapse load multipliers and safety factors for the Amatrice case study.  
 797

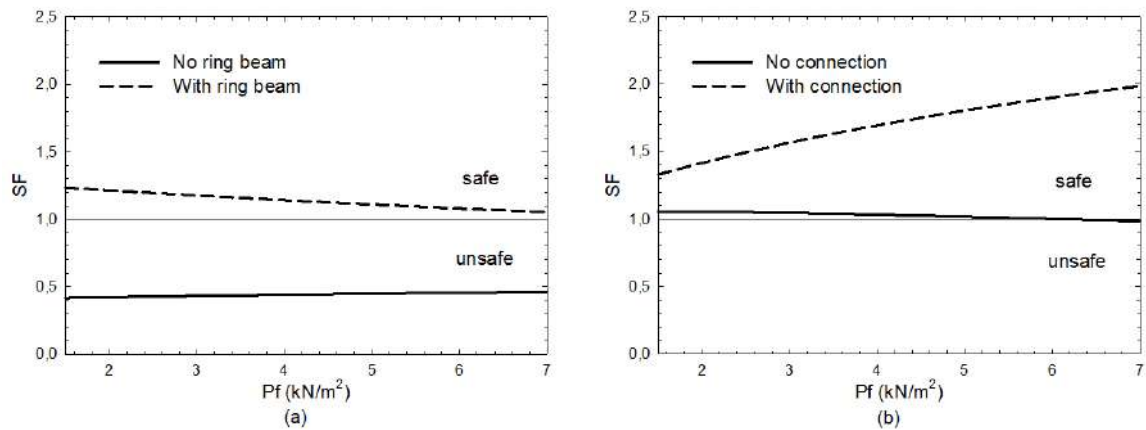
	2-storey overturning without ring beam	2-storey overturning with ring beam	2-storey vertical flexural behaviour without connection between floor and walls	2-storey vertical flexural behaviour with connection between floor and walls
$\alpha_C$	0.06	0.16	0.16	0.27
$SF$	0.44	1.14	1.03	1.70

805 351  
 807 352 Comparing these results, it is clear that the configuration of overturning with no ring beam is  
 808 353 the less safe and the most probable. The presence of a ring beam increases the collapse load  
 809 354 multiplier of about 2.7 times for the overturning mechanism. On the other hand, the model  
 810 355 with connection at the top of the walls and at floor level is the safest and less probable case.  
 811 356 For the vertical flexural behaviour, the case with connection between floor and walls has 1.7  
 812 357 times as high of a collapse load as the case without connection has. Finally, it is possible to  
 813 358 observe that the mechanisms of overturning with ring beam and vertical flexural behaviour  
 814 359 without connection at floor level are almost equivalent.  
 815  
 816

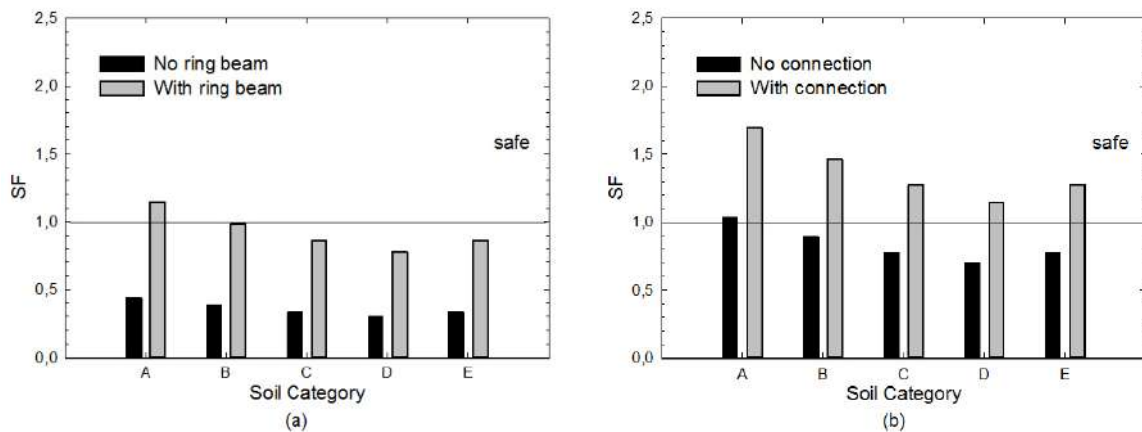
817 360 Also for this case study, sensitivity analyses were performed for all parameters. The trends of  
 818 361 variation of other parameters are really similar to the previous ones, thus the considerations  
 819 362 done for the 1-storey model are still valid. The substantial difference between 2-storey  
 820 363 overturning and vertical flexural behaviour is that in the second case the safety factors are  
 821 364 higher. Omitting obvious and well-known results, it is worth to comment what happens when  
 822 365 the floor weight is changing (Figure 11). In both cases of overturning and in the case of  
 823  
 824  
 825  
 826

827  
828  
829  
830  
831  
832  
833  
834  
835  
836  
837  
838  
839  
840  
841  
842  
843  
844  
845  
846  
847  
848  
849  
850  
851  
852  
853  
854  
855  
856  
857  
858  
859  
860  
861  
862  
863  
864  
865  
866  
867  
868  
869  
870  
871  
872  
873  
874  
875  
876  
877  
878  
879  
880  
881  
882  
883  
884  
885

366 vertical flexural behaviour without connection, when the floor weight varies the safety factor  
 367 is not subject to significant changes. A slight reduction of SF can be observed in the  
 368 overturning scenario for the model with ring beam as the floor weight increases. A heavier  
 369 floor leads to greater horizontal inertial forces which contribute to the overturning. Instead,  
 370 for the mechanism of vertical flexural behaviour with connection, a heavy floor has a positive  
 371 impact since the stabilizing force increases. As far as the variation of soil category is  
 372 concerned, the values of the  $S_s$  coefficient that were used in the previous case study are still  
 373 valid (Table 2). It is interesting to notice that if the category of soil was not “A” (rock soil),  
 374 then only the mechanism of vertical flexural behaviour with connection would be safe  
 375 (Figure 12).



376  
377 Figure 11. Floor weight vs. safety factor for the (a) overturning mechanism and the (b)  
378 vertical flexural behaviour.



380  
381 Figure 12. Soil category vs. safety factor for the (a) overturning mechanism and the (b)  
382 vertical flexural behaviour mechanism.

### 384 5. Nonlinear kinematic analysis

385 Nonlinear kinematic analyses were carried out with the aim of supporting the results obtained  
 386 from linear analyses. The whole procedure follows the method proposed by Italian codes [5,

886  
887  
888  
889  
890  
891  
892  
893  
894  
895  
896  
897  
898  
899  
900  
901  
902  
903  
904  
905  
906  
907  
908  
909  
910  
911  
912  
913  
914  
915  
916  
917  
918  
919  
920  
921  
922  
923  
924  
925  
926  
927  
928  
929  
930  
931  
932  
933  
934  
935  
936  
937  
938  
939  
940  
941  
942  
943  
944

387 6], which is presented hereafter just in its main steps. The underlying idea of the method is to  
 388 determine the trend of the horizontal action that the structure is progressively able to  
 389 withstand during the collapse mechanism's evolution. This can be seen as the capacity curve  
 390 of an equivalent single degree of freedom system. The ultimate displacement capacity of the  
 391 local mechanism is then defined and compared with the seismic demand. Similarly to the  
 392 linear case, a multiplier  $\alpha$  is introduced and defined as the ratio between the applied  
 393 horizontal forces and the displacement  $d_k$  of a control point. The horizontal multiplier of  
 394 loads is evaluated at various configurations of the kinematic chain until reaching the collapse  
 395 condition, which is identified by a null multiplier  $\alpha$ , and a displacement  $d_{k,0}$ . Assuming that  
 396 involved actions (i.e. weights, external and internal forces) are constant during the evolution  
 397 of the mechanism, the curve is almost linear. In this case, only the evaluation of the  
 398 displacement  $d_{k,0}$  is required, and the curve is described by Eq. (12):

$$\alpha = \alpha_0(1 - d_k / d_{k,0}) \tag{12}$$

400 where  $\alpha_0$  denotes the value of the multiplier capable of activating the analysed mechanism.  
 401 The problem can be solved considering a configuration varied from the static condition and  
 402 calculating the induced finite rotation  $\theta_k$  by means of virtual work principle. Reaching the  
 403 collapse situation, the overturning moment equals the stabilizing moment, and the resulting  
 404 nonlinear equation gives the final rotation  $\theta_{k,0}$ . Once the latter is determined, the  
 405 corresponding displacement  $d_{k,0}$  can be obtained. Let the control point be the center of gravity  
 406 of vertical forces, and  $h_{bar}$  be its distance from the base hinge. Eq. (13) expresses the relation  
 407 between the rotation angle and the displacement of the control point related to ultimate  
 408 capacity towards horizontal actions.

$$d_{k,0} = h_{bar} \sin \theta_{k,0} \tag{13}$$

410 At this point, it is possible to define the  $\alpha - d_k$  curve according to Eq. (12). The equivalent  
 411 capacity curve should now be determined. It describes the relation between the acceleration  
 412  $a^*$  that activates the mechanism and displacement  $d^*$ . The first is obtained through Eq. (2) as  
 413 in the linear case, whereas  $d^*$  is given by Eq. (14).

$$d^* = d_{k,0} \frac{\sum_{i=1}^{n+m} P_i \delta_{x,i}^2}{\delta_{x,k} \sum_{i=1}^{n+m} P_i \delta_{x,i}} \tag{14}$$

415 where:  $n+m$  is the number of weight forces that generates horizontal forces upon the macro-  
 416 elements;  $P_i$  is the generic weight force;  $\delta_{x,i}$  is the virtual horizontal displacement of the  
 417 application point of  $P_i$ ;  $\delta_{x,k}$  is the horizontal virtual displacement of the control point.

418 Making the same assumption done for the  $\alpha - d_k$  curve, the capacity curve can be derived from  
 419 Eq. (15).

$$a^* = a_0^*(1 - d^* / d_0^*) \tag{15}$$

421 where  $d_0^*$  is the equivalent displacement corresponding to  $d_{k,0}$ .



422 The verification for the life safety limit state consists in a comparison between the ultimate  
 423 displacement capacity  $d_u^*$  of the local mechanism and the spectral displacement evaluated at  
 424 the period  $T_s$  (Eq. (16)):

$$T_s = 2\pi \sqrt{\frac{d_s^*}{a_s^*}} \quad (16)$$

426 where  $a_s^*$ , is the acceleration correspondent to the displacement  $d_s^*$ , which is equal to  $0.4d_u^*$ ,  
 427 and  $d_u^* = 0.4d_0^*$ . Therefore, if  $d_u^*$  is greater than the spectral displacement  $S_{De}(T_s)$ , the  
 428 verification is fulfilled (Eq. (17)).

$$SF = \frac{d_u^*}{S_{De}(T_s)} \geq 1 \quad (17)$$

430 Table 4 shows obtained results for all analysed models. As expected, a lack of connection is  
 431 responsible of a small safety factor, always around 1 for the three studied cases. On the other  
 432 hand, the presence of a ring beam or floor-wall connections ensures much more capacity to  
 433 withstand larger ultimate displacements, which also means a higher safety level. The  
 434 difference is less exaggerated in the case of vertical flexural behaviour since the connection  
 435 between the floor and the wall makes the structure more rigid.

436 Comparing the linear with the nonlinear kinematic analysis in terms of safety factors, the bar  
 437 chart of Figure 13 can be plotted. The nonlinear kinematic analysis usually provides safety  
 438 coefficients that are two times or more the coefficient obtained with the linear analysis. This  
 439 confirms that a fast and preliminary analysis, such as the linear one, provides precautionary  
 440 results and it is recommended to understand if further investigations are needed. The  
 441 described trend is inverted in the cases of vertical flexural behaviour, although the nonlinear  
 442 safety factors are just slightly lower than linear ones. This phenomenon is due to the fact that  
 443 the weight of a reinforced concrete roof has a particularly positive effect for these two  
 444 models. In addition, the same analyses were repeated several times increasing the weight of  
 445 the roof for each iteration. In all cases the safety factor increased, but the increment in the  
 446 linear analysis was greater than in the nonlinear one.

447 Table 4. Results of the nonlinear kinematic analysis.

	Pescara del Tronto		Amatrice			
	1-storey overturning without ring beam	1-storey overturning with ring beam	2-storey overturning without ring beam	2-storey overturning with ring beam	2-storey flexural behaviour without connection	2-storey flexural behaviour with connection
$d_u^*$ [m]	0.089	0.227	0.093	0.326	0.041	0.074
$SF$	1.04	2.66	1.02	3.02	1.12	1.95

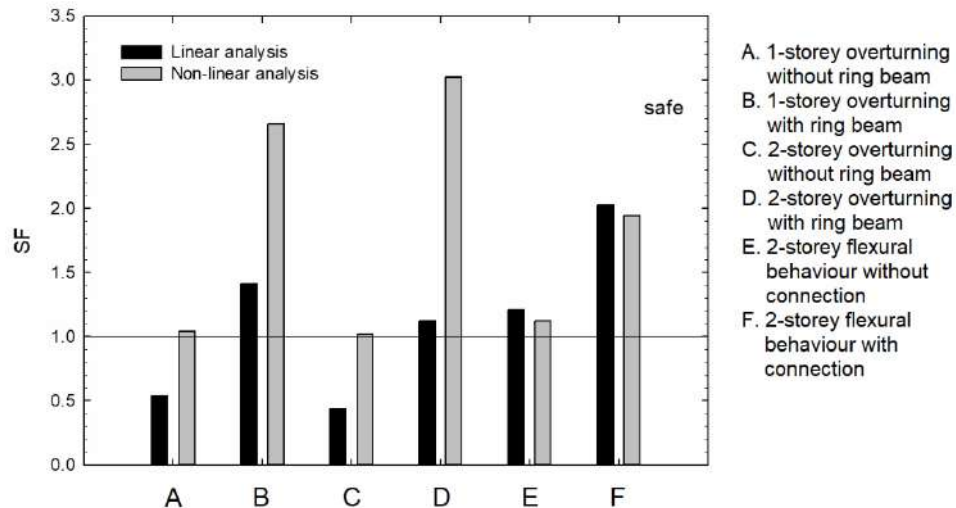


Figure 13. Comparison between safety factors resulting from linear and non-linear analyses.

## 6. Conclusions

The 2016 Central Italy earthquake caused damages and collapses of many masonry buildings, including those retrofitted with reinforced concrete roofs. This type of retrofit intervention seems to facilitate some collapse mechanisms if not properly executed. The paper presents a simplified procedure to evaluate the seismic performance of masonry buildings retrofitted with reinforced concrete roofs based on the linear kinematic analysis. Despite the analysis method is well known, the proposed models have the advantage of explicitly considering the interaction between the roof and the walls. Moreover, they require only few input parameters that can be easily obtainable. The collapse load multiplier obtained as output of the linear kinematic analysis was used to define a safety factor to have an idea whether a structure can be considered safe towards a certain collapse mechanism.

The introduced analytical models are based on the overturning and vertical flexural behaviour collapse mechanisms. In particular, the overturning scenario was analysed both for a 1-storey and a 2-storey building, while the vertical flexural behaviour was considered for a 2-storey building. Each scenario is studied twice: one configuration assuming that there is no connection among the involved macro-elements and another one that provides for an effective connection. The resulting six models were applied to two case studies, a 1-storey and a 2-storey building both collapsed during the 2016 Central Italy earthquake. Results highlight the importance of an efficient connection between the reinforced concrete roof and masonry walls and that some configurations are unsafe, which means additional investigations and possibly retrofit intervention are required. To account for the uncertainties introduced by the simplified models, sensitivity analyses were performed. These allowed to evaluate the influence of each input parameter to the overall safety level of the structure, highlighting peculiar aspects in each mechanism. Nonlinear kinematic analyses were also carried out and results were compared to those obtained from linear analyses. It was possible to observe that the linear analysis is faster and more precautionary as it provides smaller safety factors with respect to the nonlinear one.



Overall, the proposed analytical models represent an effective yet simple tool that can serve as a preliminary evaluation of the safety level of masonry structures retrofitted with reinforced concrete roofs. The method is not meant to be an alternative to other more refined analyses, such as finite element methods, that would allow for a more accurate safety verification. However, due to its simplicity, the procedure could be recommended when only few input data are available and be applied even by non-professional users to understand if further investigations and/or retrofit interventions are needed.

## Acknowledgement

The research leading to these results has received funding from the European Research Council under the Grant Agreement n. ERC\_IDEAL RESCUE\_637842 of the project IDEAL RESCUE\_Integrated Design and Control of Sustainable Communities during Emergencies.

## References

- [1] “DM 16-01-1996. Norme tecniche per le costruzioni in zone sismiche”. 1996. Ministero dei Lavori Pubblici: Gazzetta Ufficiale.
- [2] Calderini, C. 2008. “Use of reinforced concrete in preservation of historic buildings: conceptions and misconceptions in the early 20th century”. *International Journal of Architectural Heritage*, 2(1): 25-59.
- [3] Dolce, M., A. Masi, and A. Goretti. 1999. *Damage to buildings due to 1997 Umbria-Marche earthquake*. Seismic Damage to Masonry Buildings, ed. A. Bernardini. Leiden: A a Balkema Publishers. 71-80.
- [4] Donati, S., F. Marra, and A. Rovelli. 2001. “Damage and ground shaking in the town of Nocera Umbra during Umbria-Marche, central Italy, earthquakes: The special effect of a fault zone”. *Bulletin of the Seismological Society of America*, 91(3): 511-519.
- [5] “DM 14-01-2008. Norme tecniche per le costruzioni”. 2008. Ministero dei Lavori Pubblici: Gazzetta Ufficiale.
- [6] “Circolare 2 febbraio 2009, n. 617 Istruzioni per l'applicazione delle «Nuove norme tecniche per le costruzioni»”. 2009. Ministero delle Infrastrutture e dei Trasporti.
- [7] Chen, Z.X., et al. 2016. “Nonlinear Analysis of Masonry Buildings Under Seismic Actions with a Multifan Finite Element”. *International Journal of Structural Stability and Dynamics*, 16(1).
- [8] Valente, M. and G. Milani. 2016. “Non-linear dynamic and static analyses on eight historical masonry towers in the North-East of Italy”. *Engineering Structures*, 114: 241-270.
- [9] Milani, G. 2011. “Simple lower bound limit analysis homogenization model for in- and out-of-plane loaded masonry walls”. *Construction and Building Materials*, 25(12): 4426-4443.
- [10] Milani, G. and M. Valente. 2015. “Comparative pushover and limit analyses on seven masonry churches damaged by the 2012 Emilia-Romagna (Italy) seismic events: Possibilities of non-linear finite elements compared with pre-assigned failure mechanisms”. *Engineering Failure Analysis*, 47: 129-161.

1122  
1123  
1124  
1125  
1126  
1127  
1128  
1129  
1130  
1131  
1132  
1133  
1134  
1135  
1136  
1137  
1138  
1139  
1140  
1141  
1142  
1143  
1144  
1145  
1146  
1147  
1148  
1149  
1150  
1151  
1152  
1153  
1154  
1155  
1156  
1157  
1158  
1159  
1160  
1161  
1162  
1163  
1164  
1165  
1166  
1167  
1168  
1169  
1170  
1171  
1172  
1173  
1174  
1175  
1176  
1177  
1178  
1179  
1180

[11] Arcidiacono, V., G.P. Cimellaro, and J.A. Ochsendorf. 2015. "Analysis of the failure mechanisms of the basilica of Santa Maria di Collemaggio during 2009 L'Aquila earthquake". *Engineering Structures*, 99: 502-516.

[12] Arcidiacono, V., et al. 2016. "The Dynamic Behavior of the Basilica of San Francesco in Assisi Using Simplified Analytical Models". *International Journal of Architectural Heritage*, 10(7): 938-953.

[13] Casapulla, C. and A. Maione. 2011. "Out-of-plane local mechanisms in masonry buildings. the role of the orientation of horizontal floor diaphragms". *Proceedings of the 9th Australasian Masonry Conference*: 225-235.

[14] Costa, A.A., et al. 2012. "Out-of-plane behaviour of existing stone masonry buildings: experimental evaluation". *Bulletin of Earthquake Engineering*, 10(1): 93-111.

[15] Guadagnuolo, M., A. Donadio, and G. Faella. 2012. *Out-of-plane failure mechanism of masonry building corners*. Structural Analysis of Historical Constructions, Vols 1-3., ed. J. Jasienko. Structural Analysis of Historical Constructions, Vols 1-3. 481-488.

[16] Makris, N. 2014. "The role of the rotational inertia on the seismic resistance of free-standing rocking columns and articulated frames". *Bulletin of the Seismological Society of America*, 104(5): 2226-2239.

[17] Makris, N. and M.F. Vassiliou. 2014. "Dynamics of the rocking frame with vertical restrainers". *Journal of Structural Engineering*, 141(10): 04014245.

[18] Giresini, L., M. Fragiaco, and M. Sassu. 2016. "Rocking analysis of masonry walls interacting with roofs". *Engineering Structures*, 116: 107-120.

[19] Borri, A., G. Castori, and A. Grazini. 2009. "Retrofitting of masonry building with reinforced masonry ring-beam". *Construction and Building Materials*, 23(5): 1892-1901.

[20] Guadagnuolo, M. and G. Faella. 2015. "Floor masonry beams reinforced by BFRG Innovation on advanced composite materials for strengthening of masonry structures", in *XIII Forum Internazionale di Studi "Le Vie dei Mercanti"–HERITAGE and TECHNOLOGY MIND KNOWLEDGE EXPERIENCE*. La scuola di Pitagora editrice, pp. 2108-2115.

[21] Fayala, I., O. Limam, and I. Stefanou. 2016. "Experimental and numerical analysis of reinforced stone block masonry beams using GFRP reinforcement". *Composite Structures*, 152: 994-1006.

[22] Derakhshan, H., et al. 2014. "In situ out-of-plane testing of as-built and retrofitted unreinforced masonry walls". *Journal of Structural Engineering*, 140(6): 04014022.

[23] Boscato, G., et al. 2014. "Seismic Behavior of a Complex Historical Church in L'Aquila". *International Journal of Architectural Heritage*, 8(5): 718-757.

[24] Casapulla, C. and L.U. Argiento. 2016. "The comparative role of friction in local out-of-plane mechanisms of masonry buildings. Pushover analysis and experimental investigation". *Engineering Structures*, 126: 158-173.